University of Wales Trinity Saint David

School of Engineering

Determining the Relevance of the MIRA Reference Geometries to the Modern Automotive Design Process

Abstract: The project focused on determining the relevance of the MIRA reference geometries to the modern automotive design process. The Ahmed body and MIRA notchback shapes were used in conjunction with the ANSYS CFD software package to generate a calibrated CFD simulation environment suitable for testing other shapes. The MIRA notchback, estate, fastback and pickup geometries were tested in the calibrated environment and results were attained. Following this, the Solidworks CAD package was used to produce aerodynamic elements; a front air dam and rear spoiler of differing heights. The elements produced were then tested whilst attached to the notchback geometry to see if aerodynamic components produced the same effects on a MIRA reference geometry as would be expected from a commercially produced vehicle. The results from the four different MIRA reference geometries matched with existing literature. However, that confirmed how different the geometries were from modern vehicles and thus, how irrelevant to the modern design process they currently are. Both the air dam study and the rear spoiler study produced results that did not correspond with expectations. As with the preceding study on the MIRA geometries, the shape and design of the geometries themselves was the cause. Having conducted all testing and analysis, it was clear that the MIRA reference geometries both in their own right, and as testing platforms for aerodynamic elements, lack relevance to the modern automotive design process. However, their suitability for both calibration and academic purposes was clear as they allowed for the calibration of software to be streamlined.

Oscar Hardwick

BEng Motorsport Engineering

2019

Declaration of Authenticity

This thesis is the result of the author's original research. It has been composed by the author and has not been previously submitted for examination which has led to the award of a degree.

Signed: Date:

Acknowledgement

I would like to thank Dr Tim Tudor for supervising on this project, and his continued support and assistance.

Main Body Word Count: 10,521

Table of Contents

1. Aims and Objectives 1
1.1 General Aims 1
1.2 Specific Aims 1
1.3 Objectives to Achieve Specific Aim 1 1
1.4 Objectives to Achieve Specific Aim 2 1
1.5 Objectives to Achieve Specific Aim 3 2
2. Timing Plan 3
3. Literature Review 4
3.1 History of Aerodynamics 4
3.2 Aerodynamics in a Wider Context 6
3.3 Modern Aerodynamic Development 8
3.4 MIRA Reference Geometries 10
4. Methodology 12
4.1 Calibration of CFD Software 12
4.1.1 Wind Tunnel Ahmed Data 12
4.1.2 Collected Data 13
4.1.3 Ahmed Domain Size Study 13
4.1.4 Ahmed Meshing Study 14
4.1.5 Ahmed Turbulence Model Study 16
4.1.6 Further Optimization Conditions 16
4.1.7 Summary Ahmed Body CFD Settings 17
4.2 MIRA Geometry Calibration 17
4.2.1 MIRA Reference Car Information 17
4.2.2 MIRA Notchback Domain Study 18
4.2.3 MIRA Notchback Mesh Study 18
4.2.4 Summary MIRA Notchback CFD Settings 20
4.3 MIRA Geometry Comparison 20
4.4 Aerodynamic Components 21
4.4.1 Front Air Dam Study 21
4.4.2 Front Air Dam Running 21
4.4.3 Rear Spoiler Study 22
4.4.4 Rear Spoiler Running 22

5. Results 23
5.1 MIRA Geometries 23
5.2 Notchback Aerodynamic Components 31
5.2.1 Front Air Dam 31
5.2.2 Rear Spoiler 34
6. Discussion 39
6.1 MIRA Geometries 39
6.1.1 Relevance to the Modern Automotive Design Process 40
6.1.2 Potential Improvements 41
6.2 Notchback Aerodynamic Components 41
6.2.1 Front Air Dam 41
6.2.2 Rear Spoiler 42
6.2.3 Relevance to Real-World Aerodynamic Development 42
7. Conclusion 44
8. Recommended Further Work 46
8.1 Small Scale Wind Tunnel Testing 46
8.2 Increased Scope 47
8.3 MIRA Reference Redesign 47
9. References 48

Table 1- Ahmed Drag and Lift Coefficients. 12
Table 2- Ahmed Study Run Settings 13
Table 3- Summary Ahmed Body Settings. 17
Table 4- Target Notchback Coefficients 19
Table 5- Summary MIRA Notchback CFD Settings. 20

Figure 1- Turbulence Models.. 10
Figure 2- Percentage Difference to Real-World Cl Value. 14
Figure 3 - Cumulative Percentage Difference of Specific Run to Target Ahmed values for Cl and Cd. (Runs 3 and 4) 14
Figure 4 - Cumulative Percentage Difference of Specific Run to Target Ahmed values for Cl and Cd. (Runs 5 through 7) 15
Figure 5 - Cumulative Percentage Difference of Specific Run to Target Ahmed values for Cl and Cd. (Runs 8, 9 and 12) 16
Figure 6- MIRA Reference Geometries. 18
Figure 7- Notchback Calibration Runs Compared to Real-World Values (Cd). 19
Figure 8- Notchback Calibration Runs Compared to Real-World Values (Cl). 20
Figure 9 - Example of Front Air Dam added to Notchback Geometry 21
Figure 10 - Example of Rear Spoiler on the Notchback Geometry 22
Figure 11- Mira Geometries Drag and Lift Coefficients. 23
Figure 12 - Air Pressure Contours, Notchback and Fastback. 25
Figure 13- Air Pressure Contours, Pickup and Estate. 27
Figure 14- Air Velocity Contours, Notchback and Fastback. 28
Figure 15- Air Velocity Contours, Pickup and Estate 30
Figure 16- Front Air Dam Drag and Lift Coefficients. 31
Figure 17- Air Pressure Contours, Front Air Dam. 32
Figure 18- Air Velocity Contours, Front Air Dam. 33
Figure 19- Rear Spoiler Drag and Lift Coefficients. 34
Figure 20- Air Pressure Contours, Rear Spoiler. 35
Figure 21- Air Velocity Contours, Rear Spoiler. 37
Figure 22 - 3D Printed MIRA Reference Geometry in Small Scale Wind Tunnel. 46

1. Aims and Objectives

1.1 General Aims

The general aim of this project is to determine how the shape of a vehicle can affect both its lift and drag, with MIRA reference geometries and CFD utilised for the assessment. In addition, common aerodynamic components will be added to a vehicle to establish their effect on drag and lift, and how these results compare to real-world values.

1.2 Specific Aims

1 – To develop a validated CFD model of the MIRA notchback geometry using methods previously determined through an Ahmed body study.

Formatted: Justified

2 – Compare the drag and lift coefficients and air flow structures of the different MIRA reference geometries.

3 – Design and attach aerodynamic components to the notchback geometry to show how they affect the lift, drag, and air flow.

1.3 Objectives to Achieve Specific Aim 1

1 – Complete software calibration using the Ahmed body and other relevant parameters derived from previous studies.

2 – Apply these calibration settings to the MIRA notchback geometry, making necessary alterations to achieve calibration reflective of real-world values.

3 – Attain a complete and calibrated simulation environment for use with the notchback and other MIRA reference geometries.

1.4 Objectives to Achieve Specific Aim 2

1 – Run CFD simulations on all MIRA reference geometries within the previously calibrated simulation environment.

2 – Collate results from completed runs.

3 – Compare and analyse these results in terms of the drag and lift coefficients of each MIRA geometry.

4 – Compare and analyse the differing air flow characteristics of each MIRA geometry.

1.5 Objectives to Achieve Specific Aim 3

1 – Use suitable computer aided design (CAD) software to design and attach aerodynamic elements to the MIRA notchback shape.

2- Run CFD simulations on the notchback geometry and added aerodynamic elements within the previously calibrated simulation environment.

3 – Compare and analyse how the addition of aerodynamic components alters the drag and lift coefficients and air flow characteristics of the notchback.

2. Timing Plan

TIMESCALES

2017											
Week Commencing	09-Oct	16-Oct	23-Oct	30-Oct	06-Nov	13-Nov	20-Nov	27-Nov	04-Dec	11-Dec	18-Dec	25-Dec
Project Proposal												
CFD Software Learning Time												
Progress Seminar (Poster)												
Literature Survey												
Interim Viva (Assessed Work)												
Ahmed Body Study												
	Break in Studies 2018											

Key :	
Working on Task =	
Task Deadline =	
Draft/ Proofing =	

2019																		
Week Commencing	31-Dec	07-Jan	14-Jan	21-Jan	28-Jan	04-Feb	11-Feb	18-Feb	25-Feb	04-Mar	11-Mar	18-Mar	25-Mar	01-Apr	08-Apr	15-Apr	22-Apr	29-Apr	06-May
Calibrate Software for Notchback																			
CFD Simulation: MIRA Geometries																			
CAD Aerodynamic Component Design																			
CFD simulation: Aero Components																			
Results and Analysis																			
Final Report (Assessed Work)																			
Final Viva (Assessed Work)																			

WORK PLAN

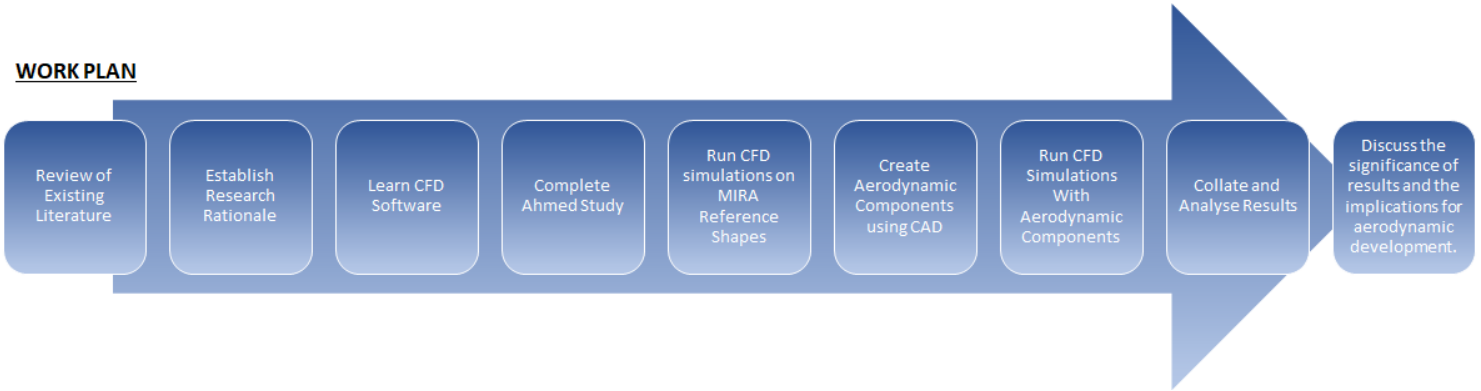

3. Literature Review

Aerodynamics is defined as, “The science that studies the movement of gases and the way solid bodies, such as aircraft, move through them” (Cambridge Dictionary, 2019). This project will focus on the process by which aerodynamics can be studied, as well as how the results deduced from computational fluid dynamic analysis can be applied in both automotive and motorsport scenarios. By using generic vehicle shapes developed by MIRA and testing those shapes in modern CFD software to study how air flows over them, valuable information can be collected that may inform real-world vehicle development.

To fulfil the aims and objectives detailed in Section 1, a review of existing literature is needed to give background context to the study and establish an understanding of key concepts.

3.1 History of Aerodynamics

The study of aerodynamics first began in the 18th Century, with pioneers such as Daniel Bernoulli and Isaac Newton developing the empirical foundations upon which modern day aerodynamics is built. Bernoulli in particular was the first to experiment with fluid mechanics, and managed to describe the relationship between pressure, velocity and density that we still use in the present day to determine lift values (Dietz & Heesterbeek, 2002), as well as to develop new aerodynamic designs and components. Having established key relationships and forces, the focus in respect to applying these new theories and principles first concentrated on achieving heavier than air flight. The initial concept for heavier than air flight and fixed wing aircraft came from George Cayley in the very late 18th Century and early 19th Century (Gibbs-Smith, 1962), and by the early 20th Century, Wilbur and Orville Wright became the first men to successfully achieve heavier than air flight (Jakab, 2014). Following the application of aerodynamic principles to the development of aircraft, attention then turned to utilizing these principles on motor vehicles.

When cars became widely available in the early 20th Century, speed and performance quickly came to the forefront of road vehicle design. For a number of years, the focus lay almost entirely on outright speed. Designers and manufacturers became competitive with one another across several fields, the key of which was the land speed record. Early endeavours focused solely on increasing power output as a way to gain speed, but this had limitations due to the engine technology and resources available at the time (Posthumus & Tremayne, 1985). As opposed to looking only at increasing power, designers then started working on reducing drag and experimenting with aerodynamics, to discover how something

originally used to get us off of the ground, could help us go much faster along it. Therefore, in the early years of performance cars and motorsport competition, going quickly was all about reducing drag and increasing power (Earl, 1947). It wasn't until the 1960s, when the worlds of both Formula 1 and sportscar racing began to use aerodynamics in their now most popular application in motorsports, to produce downforce.

Whilst Opel had used inverted aircraft wings in the 1920s on a rocket car to avoid issues with taking off (Darling, 2016), the idea of using downforce as an aid to performance didn't become popular until the 1960s. In Formula 1, Bruce McLaren initially toyed with the concept of wings and downforce in the very early parts of the decade, but Colin Chapman of Lotus really pushed the concept in to the mainstream of the racing world (Katz, 1995). In 1962 Jim Hall and Hap Sharp founded the Chaparral Cars Company in the USA. Between 1963 and 1970 the pair worked at the very cutting edge of downforce design, going on to create the controversial 2J "fan car", which was very quickly outlawed due to its overwhelming dominance in the Can-Am class in which it was designed to compete. The 2J pioneered a phenomenon known as the ground effect. The ground effect relies entirely on Bernoulli's principle, which states that, as the area through which air can travel decreases, the velocity of the air through that area will increase, and thus cause the pressure to drop (Katz, 2006). Fans installed on the 2J allowed for the velocity of air underneath the car to be controlled, and thus a constant level of downforce maintained.

It took a while longer for the ground effect to take hold in Formula 1. In 1977 Colin Chapman headed a team of designers who brought the ground effect to the forefront of the Formula 1 field with the Lotus 78, which immediately won races and forced a change in approach amongst the whole Formula 1 field (Katz, 2006). The ground effect, whilst efficient and advantageous to a cars performance, came with a list of drawbacks, key of which was a lack of safety. This safety issue was born mostly out of there being few ways to effectively test designs. Most teams who aimed to copy Lotus did so by eye for the most part, which led to existing issues with the phenomenon being exaggerated even further. This led to the development of the ground effect, and ground effect related design components, being outlawed within Formula 1 and beyond, due to the safety concerns associated with it (Zhang et al, 2006). From the early 1980s onwards, a dedication to testing and understanding of aerodynamic design came to the forefront of the motorsports world and helped spur on the emerging technologies that could aid the design process, such as wind tunnels, computer aided design (CAD) and computational fluid dynamics (CFD). Currently, the necessity and usage of advanced wind tunnels, CAD and CFD are crucial mainstays of the aerodynamic design process, not only in the world of motorsports, but also in the world of manufacturing day to day road vehicles in the automotive industry (Groover & Zimmers, 1983).

3.2 Aerodynamics in a Wider Context

Aerodynamics is commonly defined as the study the flowing of gases over a solid body to determine how said body will react. Whether it be for the development of aircraft, cars, bikes or boats, the use of aerodynamics is crucial to an optimized and complete design process. With any of these mentioned applications, the use of basic gas flow values, calculations, and fundamentals must be understood and utilized to achieve the best results. The study of aerodynamics relies largely on the calculation and understanding of two key forces, drag and lift. When looking at airflow over any solid body, lift accounts for the vertical forces created by airflow over the body, whilst drag accounts for all forces acting horizontally that impede forward motion (Katz, 2006).

The drag on a motor vehicle is caused by a build-up of high pressure at the front of a vehicle, and the comparative low pressure that accumulates behind it (Altinisik, 2017). This differential forms a relative 'vacuum' behind the body which pulls, or sucks, against the direction of travel. Another component of drag is frictional drag. Frictional drag makes up a far smaller part of the drag forces acting on a body compared to the air pressure differences, but is nonetheless important to good aerodynamic design, especially in the aeronautical industry where the margins being worked within are incredibly fine. Frictional drag is where air flowing over a body loses energy as heat, due to friction with the body itself. As the air loses energy it can separate, and the airflow can move away from the body it is travelling over and cause further drag (McBeath, 2015).

When considering the lift acting on a body, the key principal to consider is the Bernoulli effect (Dietz & Heesterbeek, 2002). This effect states that, if the velocity of airflow over a body increases, then the pressure of that air will decrease and create a relative pressure gradient compared to the body's surroundings. By creating a lower air pressure below a body than the air pressure present above it, the air will try to move from the area of high pressure to the area of low pressure. This movement of air will cause a force that pushes the body in to the ground, referred to as either downforce or negative lift. When developing a motor vehicle, more downforce is designed in for high performance vehicles, whereas civilian road vehicles tend to produce small amounts of lift instead.

The forces for both drag and lift use calculations revolving around the coefficients of said forces.

The equation for lift force is:

$$F_L = \frac{1}{2} C_L \rho v^2 A$$

F_L is the lift force and the value that is considered when determining the downforce or lift being produced over any particular body. C_L, or the coefficient of lift, is a dimensionless coefficient that works in relation to air density, velocity, and the area over which both are acting, to help determine an accurate value for the overall force. ρ, or rho, is a symbol that denotes pressure. In the case of aerodynamics, this will normally be the pressure of the air flowing around a body. Rho can also show the pressure of any fluid in any relevant equation. v is the velocity of the air, whilst A is used to determine the total cross-sectional area that the airflow is acting over. By using the above formula, the lift force can be found, and a body can be shown to either produce lift force or downforce.

The equation for drag is:

$$F_D = \frac{1}{2} C_D \rho v^2 A$$

This equation is largely the same as that used for determining lift force. Where previously the coefficient was of lift, here it is the coefficient of drag (C_D). This equation is used to determine the forces acting horizontally on a body as opposed to vertically.

Another key factor of complex air flow around any given body is that of boundary layers and air flow separation. These two phenomenon are intrinsically linked. A boundary layer creates friction between the surface of the body and the air flowing over it. As such, it makes it less likely for the air flow moving over the body to separate, or move away from the body, and generate turbulence (Le Good et al, 1998). The design of any given body or component will aim to optimise its own boundary layer in such a way as to increase the amount of smooth air flow, or laminar air flow, over itself whilst also reducing turbulent flow in the same areas. Separation is where air flow over a body has forces in one direction that exceed the forces of friction coming from the boundary layer. When this happens, the air flow moves away from the main body in to open air and changes from a laminar to a turbulent flow. If turbulent flow was, for example, to build up behind any given body in excess, a great deal of drag would be produced (Katz, 2006). This is due to the turbulent flow moving much more slowly, sometimes even against the direction a body is moving in and building up an area of low or “negative” pressure. The delta in pressure experienced at this point, between the front and rear of the body, generates a great deal of drag. Therefore, the design process of any body, component or shape has to focus intensely on boundary layers and their suitable optimisation in order to limit the amount of separation occurring on the surface (McBeath, 2015).

When developing aerodynamic components or determining the aerodynamic behaviours of a vehicle, both the drag and lift forces must be considered. Generally speaking, the same components and designs that generate downforce or negative lift also generate higher levels of drag. The aim will always be to strike the best possible balance between the drag and lift values. Very large amounts of downforce are great on paper, however, too much may generate a level of drag too high for the thrust, or power, of a vehicle to suitably overcome. Particularly in regard to developing aerodynamic components for a motorsports vehicle, this all has to be carefully considered (Abdel-Rahman et al, 2016). There will come a point where the downforce and drag generated are so much that a vehicle becomes slower, as the maximum achievable speed is reduced dramatically by the increased drag (George, 2014). Using the above equations and CFD programs, a good balance can be struck, and the best possible components designed and produced.

3.3 Modern Aerodynamic Development

Once the importance of aerodynamics in relation to motor vehicle performance was understood, research and development of aerodynamics truly took off. Wuniblad Kamm is credited with having designed and engineered the first commercially used automotive wind tunnel in the early 1930s. Having seen the complex effect airflow over vehicles had, Kamm went on to build a much larger and more complex system in the late 30s and used it to further investigate aerodynamic effects on motor vehicles. This wind tunnel was purchased in the 1950s by Mercedes-Benz and used in a much wider commercial context. Wind tunnels remain crucial to any vehicle design and development programs (Earl, 1947). Whilst modern computer simulation can very accurately estimate air flow characteristics a wind tunnel can still form a better representation of the real-world. In addition, wind tunnels have developed over time to become incredibly close to real-world in their environments (Gaylard et al, 1998). The Sauber developed wind tunnel, used primarily in formula one aerodynamic development, uses a rolling road and fully closed system to more accurately simulate real-world air flow.

Commented [EH1]: Expand a bit on why wind tunnels are so useful and what they were created to acheive rather than just who created them first.

When powerful computers and computer programs were not widely available, the wind tunnel dominated the world of aerodynamic development for many years. However, as computers were improved and introduced in to the engineering workplace, the approach to aerodynamic development changed dramatically.

Presently, the use of computer aided design (CAD) and computation fluid dynamics (CFD) software are key factors in the design and development process of any aerodynamic engineering project. By starting the development cycle of new vehicles or components in a

computer simulation environment a huge amount of time and money can be saved. This is down to modern simulation software operating at such a level of accuracy that results attained on a computer will carry a huge amount of value in to the real world. Companies looking to develop vehicles, components and so on can avoid the high costs of physical prototype testing throughout a project and save that for when a computer designed body is confirmed as a viable approach by any suitable software packages (Groover & Zimmers, 1983; Cyr et al, 2011).

During this project two software packages will be used to complete CAD work and CFD work respectively. For all of the CAD work the solidworks package will be used. Solidworks is a software package developed and published by Dassault Systèmes that allows for a range of complex shapes and components to be designed and built in a virtual setting. This particular software package allows for as complex or as simple a design as can be desired, from basic rectangular beams all the way through to a full working mechanical model of a motor vehicle. Solidworks is therefore a suitable software package for the purposes of this project. With abilities not only to build complex shapes but also control other parameters such as material properties and operating conditions (Ghita et al, 2012), Solidworks will provide full functionality for all 3D modelling aspects of the project. CFD work will be completed using the ANSYS software package. ANSYS is a software package developed and published by ANSYS inc. This software package is designed to allow for fluid flow analysis. Whether that be a very viscous fluid like water through a pipe system, or air over an automobile, ANSYS as a package is designed to simulate any situation involving fluid flow effectively. Numerous authors have utilised ANSYS to perform CFD studies, due to its functionality and scope. Parab et al (2014) utilised the software to comprehensively test air flow over a motor vehicle. In doing so, all elements relevant to air flow simulation within the ANSYS software package were utilized. Following the same process used in similar studies such as this should allow for successful implementation of the ANSYS software in this project (Musa & Patel, 2016; Gaylard et al, 2007; Chainani & Perera, 2008)

The most complex element to be considered not only for this project, but during any project that requires the use of CFD software packages, is turbulence models. A number of models for turbulence exist but are not optimized for all situations (Soares & De Souza, 2015). For the purposes of this project the k-e realizable turbulence model will be used as various studies conducted on the Ahmed and MIRA shapes have shown it to be most effective (Howell et al, 2013; Zhang et al, 2014; Sharma & Bansal, 2013)

Commented [EH2]: Again, is there onethat is best or that yo ar using for a particular reason. what have people used in the literature?

Model	Description
Spalart – Allmaras	A single transport equation model solving directly for a modified turbulent viscosity. Designed specifically for aerospace applications involving wall-bounded flows on a fine near-wall mesh. FLUENT's implementation allows the use of coarser meshes. Option to include strain rate in k production term improves predictions of vortical flows.
Standard k–ε	The baseline two-transport-equation model solving for k and ε. This is the default k–ε model. Coefficients are empirically derived; valid for fully turbulent flows only. Options to account for viscous heating, buoyancy, and compressibility are shared with other k–ε models.
RNG k–ε	A variant of the standard k–ε model. Equations and coefficients are analytically derived. Significant changes in the ε equation improves the ability to model highly strained flows. Additional options aid in predicting swirling and low Reynolds number flows.
Realizable k–ε	A variant of the standard k–ε model. Its "realizability" stems from changes that allow certain mathematical constraints to be obeyed which ultimately improves the performance of this model.
Standard k–ω	A two-transport-equation model solving for k and ω, the specific dissipation rate (ε / k) based on Wilcox (1998). This is the default k–ω model. Demonstrates superior performance for wall-bounded and low Reynolds number flows. Shows potential for predicting transition. Options account for transitional, free shear, and compressible flows.
SST k–ω	A variant of the standard k–ω model. Combines the original Wilcox model for use near walls and the standard k–ε model away from walls using a blending function. Also limits turbulent viscosity to guarantee that $\tau_T \sim k$. The transition and shearing options are borrowed from standard k–ω. No option to include compressibility.
Reynolds Stress	Reynolds stresses are solved directly using transport equations, avoiding isotropic viscosity assumption of other models. Use for highly swirling flows. Quadratic pressure-strain option improves performance for many basic shear flows.

Figure 1- Turbulence Models. (Fluent User Services Centre, 2006).

The vast majority of geometries that will be used as a part of this project have been studied at length previously. Therefore, finding suitable turbulence models for them will not be a process of elimination, but rather a case of applying existing knowledge from suitable literature to each individual case.

3.4 MIRA Reference Geometries

One of the key objectives of this project is to validate MIRA reference cars and provide evidence that each generic geometry has very useful real-world applications. MIRA, formerly known as the Motor Industry Research Association, developed these reference geometries as a means of testing how efficient various generic vehicle designs were aerodynamically. Since being introduced, a huge number of private companies and academic institutions have used these reference geometries as the basis for research and for engineering design projects. Whilst none of these geometries are exact representations of existing road going automobiles, they represent common vehicle types meaning the information derived from testing can inform the design philosophy of new vehicles. For example, (Parab et al, 2014) found that the estate car geometry produces a much higher coefficient of drag over the notchback, or saloon car shape. Consequently, when companies design estate cars the aerodynamics receives a great deal of research and development input, as the MIRA reference geometry has shown that the vehicle shape is less aerodynamically efficient than other types.

Clearly, the MIRA geometries have been invaluable to the vehicle aerodynamic design process in the past and have therefore been incorporated into this project. Several authors have previously used both MIRA and other vehicle reference shapes to inform the aerodynamic design process. Zhang et al (2014) used the MIRA geometries as a test bed for optimisation, attempting to improve the lift and drag coefficients produced by the initial geometries. Other studies have used both MIRA and SAE geometries to develop and produce brand new reference geometries that could aid and streamline the aerodynamic development process (Heft et al, 2012). Various simple reference geometries have been used both in software calibration and also to show and describe particular air flow structures and characteristics. In addition, these studied air flow structures found from testing basic reference geometries has been linked to real-world designs and their consequent improvements. (Le Good & Garry, 2004).

Commented [EH3]: Da Fuq?

Despite these previous studies largely aimed at geometry optimisation, little research has been conducted on how these geometries could provide relevant and valuable information to aid the real-world automotive design process. This includes adding different common aerodynamic elements to the reference shapes to see how the aerodynamics are altered. This represents a research gap which this project aims to fil, showing how the MIRA reference shapes provide an opportunity to inform real world design choices.

Consequently, this project will focus on how the MIRA reference geometries and just how relevant to the real-world they are. By looking in detail at how certain reference geometries react within a virtual environment in comparison to how a real vehicle would act and concentrating on whether or not basic aerodynamic elements produce the same effects on reference geometries as would be seen in a real-world environment, this study should complement to the existing literature.

4. Methodology

4.1 Calibration of CFD Software

When conducting any air flow testing using CFD software, suitable calibration must be attained. A widely accepted method for calibrating the software package being used is to carry out an Ahmed body study and match the ANSYS results with the real-world values (Govardhana & Reddy, 2014). A CFD study of any body will include examinations of the domain being tested across, the mesh within which calculations are being carried out, as well as a turbulence model study. Further optimizations can be made through the application of specific wall conditions or density boxes, which allow the mesh density to be more focussed across crucial air flow area on the body being studied. Through the use of an Ahmed body study, the ANSYS software package being utilised in this project was suitably calibrated.

4.1.1 Wind Tunnel Ahmed Data

Table 1- Ahmed Drag and Lift Coefficients.

Ahmed 25 Lift Coefficient (Cl)	0.345
Ahmed 25 Drag Coefficient (Cd)	0.299

Table 1 shows the real-world wind tunnel data for the standard Ahmed body with a 25-degree slant angle (Lienhart et al., 2002). The lift coefficient (Cl) and the drag coefficient (Cd) are the reference values that were used to calibrate the ANSYS software. The air flow velocity used to attain these values was 20 m s^{-1}, and thus the same velocity was used throughout the ANSYS testing.

4.1.2 Collected Data

Table 2- Ahmed Study Run Settings

	Meshing			Solving (Fluent)			Domain (m)			Advanced Meshing									Solutions	
	Elements	Min Orthog	Max Skewness	Turbulence Model	Solution Method	Iterations	X	Y	Z	Relevance	Smoothing	Transistion	Curvature	Max Cell Size	Min Cell Size	Inflation	Layers		Cl	Cd
Run 1	171604	0.257	0.844	Laminar	Simple	150	4	1	1	Medium	High	Slow	27.5	0.102	0.0001	--	--		4.00E-01	3.05E-01
Run 2	1894998	0.251	0.841	Laminar	Simple	150	12	4	4	Medium	High	Slow	27.5	0.102	0.0001	--	--		3.03E-01	3.09E-01
Run 3	418497	0.245	0.849	Laminar	Simple	150	9.4	2.1	2.1	Medium	High	Slow	27.5	0.102	0.0001	--	--		3.20E-01	3.15E-01
Run 4	659467	0.248	0.848	Laminar	Simple	150	9.4	2.1	2.1	Fine	High	Slow	18	0.102	0.00005	--	--		2.94E-01	2.96E-01
Run 5	1412256	0.237	0.836	Laminar	Simple	150	9.4	2.1	2.1	Fine	High	Slow	18	0.064	0.00005	--	--		3.84E-01	2.76E-01
Run 6	1662408	0.23	0.832	Laminar	Simple	300	9.4	2.1	2.1	Fine	High	Slow	18	0.064	0.00005	Y		5	2.83E-01	2.51E-01
Run 7	1882661	0.25	0.82	Laminar	Coupled	300	9.4	2.1	2.1	Fine	High	Slow	18	0.064	0.00005	Y		5	3.44E-01	2.45E-01
Run 8	1882661	0.25	0.82	Reynolds Stress	Coupled	300	9.4	2.1	2.1	Fine	High	Slow	18	0.064	0.00005	Y		5	3.76E-01	2.65E-01
Run 9	1882661	0.25	0.82	k-omega	Coupled	300	9.4	2.1	2.1	Fine	High	Slow	18	0.064	0.00005	Y		5	3.37E-01	2.71E-01
Run 10	1882661	0.25	0.82	k-epsilon STD	Coupled	300	9.4	2.1	2.1	Fine	High	Slow	18	0.064	0.00005	Y		5	3.39E-01	2.79E-01
Run 11	1882661	0.25	0.82	k-epsiilon RNG	Coupled	300	9.4	2.1	2.1	Fine	High	Slow	18	0.064	0.00005	Y		5	3.55E-01	2.62E-01
Run 12	1882661	0.25	0.82	K-epsilon Realizable	Coupled	300	9.4	2.1	2.1	Fine	High	Slow	18	0.064	0.00005	Y		5	3.52E-01	2.71E-01
Run 13	1882661	0.25	0.82	K-e Real WC-A	Coupled	300	9.4	2.1	2.1	Fine	High	Slow	18	0.064	0.00005	Y		5	3.51E-01	2.70E-01
Run 14	1882661	0.25	0.82	K-e Real WC-B	Coupled	300	9.4	2.1	2.1	Fine	High	Slow	18	0.064	0.00005	Y		5	3.61E-01	2.72E-01
Run 15	1882661	0.25	0.82	K-e Real WC-B	Coupled	300	9.4	2.1	2.1	Fine	High	Slow	18	0.064	0.00005	Y		5	3.30E-01	2.67E-01
Run 16	2796143	0.228	0.838	K-e Best_New Mesh	Coupled	300	9.4	2.1	2.1	Fine	High	Slow	18	0.064	0.00005	Y		6	3.52E-01	2.78E-01

In Table 2, all of the running completed as a part of the Ahmed body study are shown. An iterative process took settings from the most basic meshing and turbulence model to the point at which the environment was suitably optimized. At this point, the drag and lift coefficients matched well to the real-world values seen in Table 1. The following sections describe the setting changes needed to achieve this optimization.

4.1.3 Ahmed Domain Size Study

Runs 1-3 in Table 2 focus on the domain size best suited to the Ahmed body. Run 1 displays a domain size which is too small, whilst Run 2's domain size is to large. Run 3 uses a ratio recommended by Lanfrit (2005), which is 3 body lengths in front of the body and 5 behind. In addition, the body should be two body widths in the x-axis and two body heights in the z-axis. This ratio allows for all airflow to be sufficiently calculated and resolved whilst simultaneously not being so large as to unnecessarily waste computing power. Whilst the mesh settings within these runs were basic, the improvement from utilising a suitable domain size is clearly evident (Figure 2). This domain size was therefore utilised throughout CFD testing in this project.

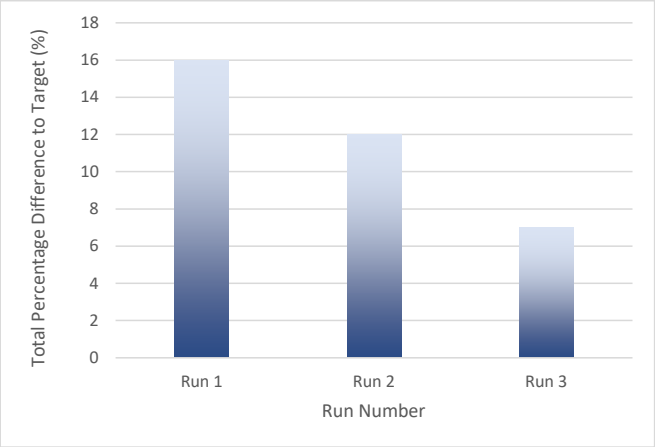

Figure 2- Percentage Difference to Real-World Cl Value.

4.1.4 Ahmed Meshing Study

The next step was to refine the mesh by altering and focussing the element density. The difference between Run's 3 and 4 show how a simple increase in general mesh density produces significant change to the lift and drag, albeit not necessarily improving the result (Figure 3).

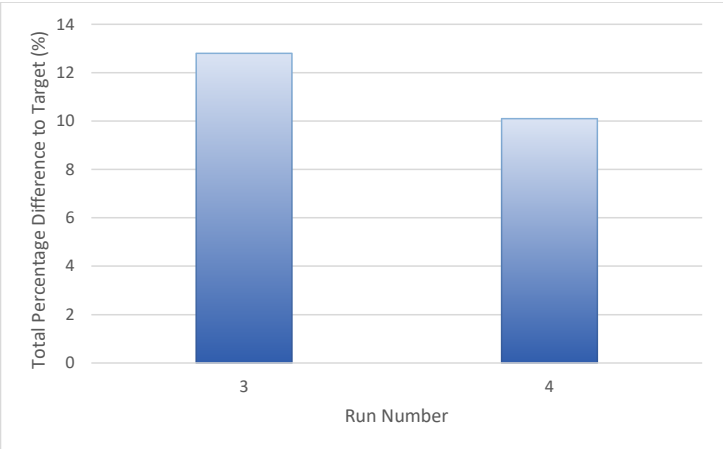

Figure 3 - Cumulative Percentage Difference of Specific Run to Target Ahmed values for Cl and Cd. (Runs 3 and 4)

Run 5 introduced a wake, or car box, to the test environment. This box allowed the mesh density over a specific area to be changed. Lanfrit (2005) recommended a wake should be at least half a body length in front of the body, and at least one length behind. Depending upon the complexity of the turbulence and the air flow velocity, an increase in the size of this box is sometimes necessitated. To determine if this is required, the turbulence can be viewed after solving in ANSYS. If the turbulence continues beyond the extent of the car box, then its size can be subsequently increased. Run 6 utilizes a larger wake box for this reason. A further alteration to the mesh which allows for more localised optimization is the addition of prism layers. Prism layers are smaller elements more rectangular in shape that sit on the surface of the body being tested. This allows for a dramatic increase in mesh density coinciding with where any boundary layers would occur. These boundary layer areas often have the most complex air flows; thus, an increased mesh density is normally required to get suitably accurate results by completing more calculations in those areas compared to others within the domain. Prism layers were introduced in Run 6 and further optimized with a more complex solution in Run 7 (Figure 4).

Commented [EH4]: Which run numbers showed tis in action.

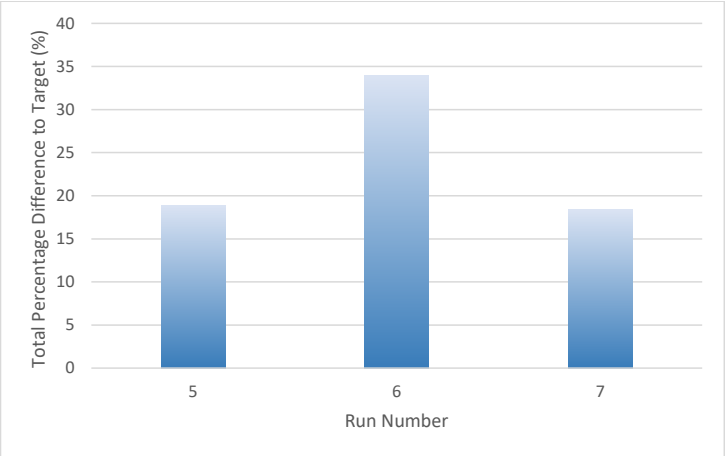

Figure 4 - Cumulative Percentage Difference of Specific Run to Target Ahmed values for Cl and Cd. (Runs 5 through 7)

Following Run 7, the testing mesh has been optimized and is unlikely to be a limiting factor in achieving accurate and valuable results.

4.1.5 Ahmed Turbulence Model Study

The turbulence model is a crucial factor when conducting an air flow study in any CFD software. Multiple different turbulence models were trialled in Runs 8-16 (Table 2), with the k-epsilon realizable model being the favoured choice (Figure 5). This is widely regarded as the most robust and reliable turbulence model when dealing not only with the Ahmed body, but any number of similar shapes that display similar turbulence structures (Banga et al, 2015)

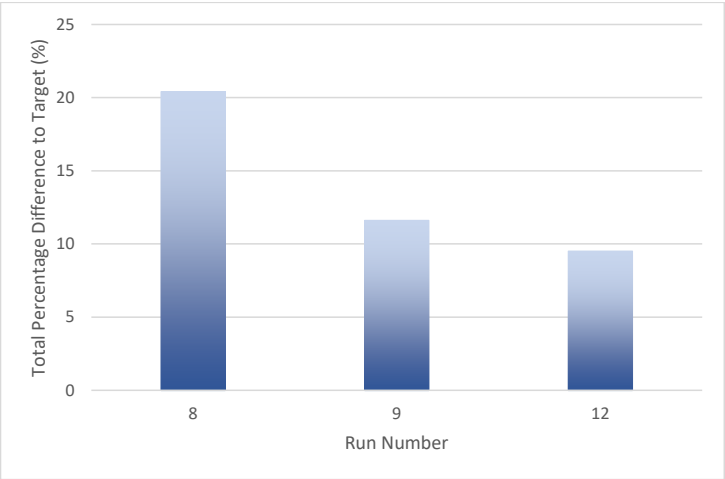

Figure 5 - Cumulative Percentage Difference of Specific Run to Target Ahmed values for Cl and Cd. (Runs 8, 9 and 12)

Figure 5 shows how much closer a result is obtained through the use of the k-e realizable model compared to two other models, in this case the Reynolds stress model and also the k-omega model respectively.

4.1.6 Further Optimization Conditions

Further aspects of the CFD test environment could be explored to improve the accuracy of the simulation verses the real-world values. The first of these to consider was wall functions. Wall functions are in affect adjustments to the turbulence model that take affect only at the walls of any given domain. This can allow for the accurate calculation of much more complex air flow structures around the walls. Literature regarding wall functions suggests the use of a scalable wall for the Ahmed and similar bodies (Banga et al, 2015). This was therefore utilised for this project, although other wall functions were tested (Table 2).

In some cases, the mesh density is not dense enough for extremely complex air flow, even when a wake box or prism layers are added. This is regularly seen underneath the body where the area between the body and a static wall, in this instance the floor, is very small. Whilst the Ahmed body arguably doesn't need an additional density box underneath the body, shapes more complex than this would likely require one. Therefore, an underbody box was added to increase accuracy slightly for this body, but more importantly added as a key feature in the meshing philosophy taken forward on to the more complex MIRA shapes assessed in this project.

4.1.7 Summary Ahmed Body CFD Settings

Table 3- Summary Ahmed Body Settings.

Solution Method	Coupled
Element Minimum Size	0.0005
Element Scale	0.75
Prism Layers	5
Domain Size	3L Forward. 5L Backward. 2H Up. 2W Side.
Turbulence Model	K-e realizable
Wall Functions	Scalable Wall
Wake Box	Yes (0.5L Forwards. 1.5L Backward. 0.5H and 0.5W)
Underbody Box	Yes

The optimized settings derived from Ahmed testing and calibration are shown in Table 3. This philosophy will be applied throughout the remaining CFD testing, with only minor alterations made to accommodate a new shape and scenario.

Commented [EH5]: is tis a technical term?

4.2 MIRA Geometry Calibration

4.2.1 MIRA Reference Car Information

The MIRA reference cars are vehicle shapes developed by MIRA to better understand how different car designs may change how air flows around them. MIRA have produced reference cars in four varieties (Figure 6): A notchback shape which is akin to a basic saloon car; an estate shape which is designed to be an estate or "wagon" version of the notchback

shape; a fastback variant designed to mimic a generic coupe vehicle shape; and a pickup variation of the notchback design, which depicts a generic pickup truck design.

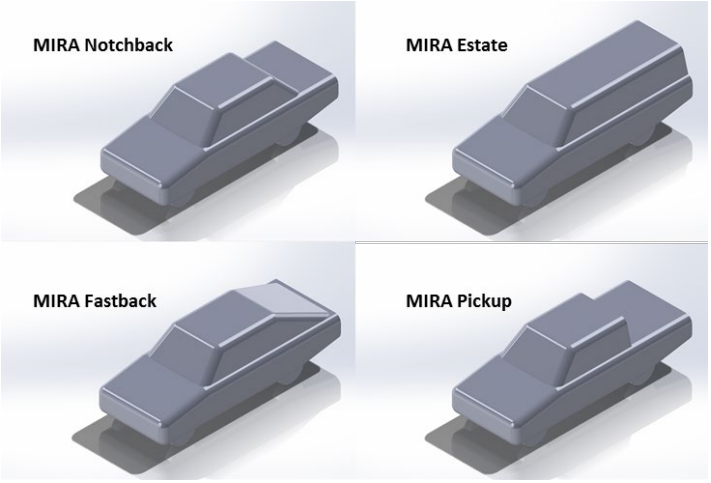

Figure 6- MIRA Reference Geometries.

None of these reference bodies are complex in their design, and it is unlikely that a real-world vehicle would look particularly similar to them. However, these bodies have been developed to show how efficient these basic shapes are when compared to one another. Automotive companies can use such information to help inform how to best design cars of certain shapes.

4.2.2 MIRA Notchback Domain Study

Using the settings established through the Ahmed body study, the domain size could quickly be produced. The ratio discussed in Section 4.1.3 was used to establish a domain that would fit the MIRA geometry. This domain was larger than that of the Ahmed body as the dimensions of the MIRA reference cars were greater. Whilst this didn't dramatically affect how the domain was built or the time taken to do so, it does foreshadow impacts that were experienced later. The larger domain size meant the element sizes and computing time of later steps needed to be altered to accommodate the new shape.

4.2.3 MIRA Notchback Mesh Study

As previously explained in Section 4.1.4, the meshing philosophy established from testing the Ahmed body can be applied to any other shape. The same turbulence model and wall functions applied to the Ahmed body were appropriate for use with the notchback, but the

physical element sizes and meshing had to undergo significant changes due to the increased domain size. Increasing the element size by a factor similar to that of the change in domain size was the most logical approach, so an element size of 0.7 was used. The element scale remained the same at 0.75. This change meant the total number of elements was similar to that used in the final runs of the Ahmed body study. The maximum element size of both the wake and underbody boxes was also adjusted accordingly, and testing of the mesh was performed.

Table 4- Target Notchback Coefficients (Palaskar et al, 2016)

Target Cd	Target Cl
0.293	-0.085

Table 4 shows the lift and drag values to be aimed for, as established by Palaskar et al (2016). Three differing runs were conducted to achieve similar values. Initially, 200 iterations were calculated. Good drag values were produced, but the coefficient of lift varied significantly from the real-world value (Figure 7 & 8). As the shape of the underside of a vehicle contributes a great deal to the Cl value, the mesh density in the underbody was increased to better calculate the airflow in and around that area. Following this change, testing showed an improvement in both lift and drag coefficients (Figure 7 & 8). A final improvement was made by increasing the iterations to 500. At this point the calibrated simulation environment was operating within 5% of the real-world drag and lift values.

Commented [EH6]: Where di you get these from?

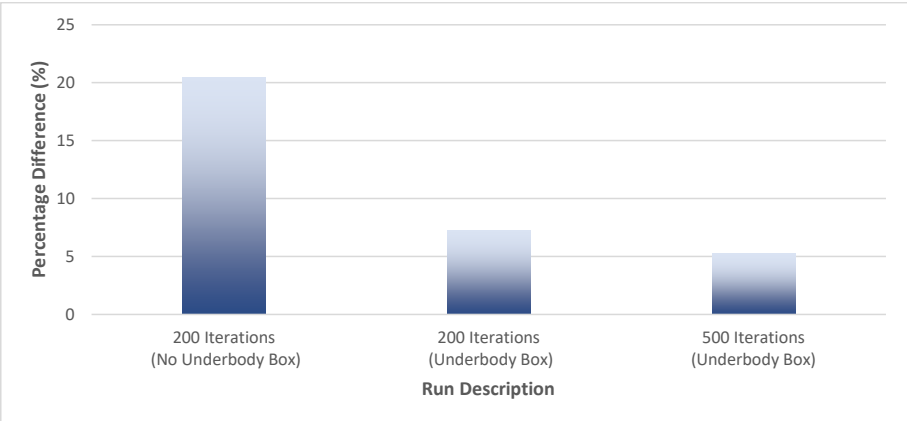

Figure 7- Notchback Calibration Runs Compared to Real-World Values (Cd).

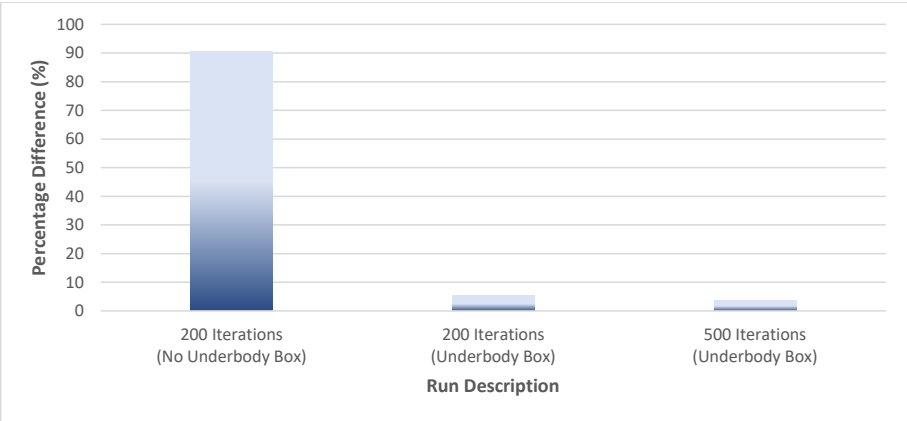

Figure 8- Notchback Calibration Runs Compared to Real-World Values (Cl).

4.2.4 Summary MIRA Notchback CFD Settings

Table 5- Summary MIRA Notchback CFD Settings.

Solution Method	Coupled
Element Minimum Size	0.7
Element Scale	0.75
Prism Layers	5
Domain Size	3L Forward. 5L Backward. 2H Up. 2W Side.
Turbulence Model	K-e realizable
Wall Functions	Scalable Wall
Wake Box	Yes (0.5L Forwards. 1.5L Backward. 0.5H and 0.5W)
Underbody Box	Yes

4.3 MIRA Geometry Comparison

Upon completion of the initial notchback running and calibration, the other MIRA reference bodies were run using the same settings. From these runs a comparison was drawn between the different geometries in terms of their drag and lift coefficients. An assessment of

how air flow differed between the different body shapes was also achieved, by utilising the pressure and velocity contour functions available in ANSYS.

4.4 Aerodynamic Components

4.4.1 Front Air Dam Study

Following comparison of the different MIRA geometries, different aerodynamic elements were added to the notchback shape to test their affects on airflow. The first element added was a front air dam. This is, in effect, a flat surface at the front of the car that decreases the area available to air moving under the vehicle. The air dam structure was created using CAD software Solidworks, with numerous different heights produced for comparison (Figure 9). The structure was then attached to the notchback shape, and CFD simulations were run using the settings outlined in Table 5. The height changed from 200-250mm, varying at 10mm intervals.

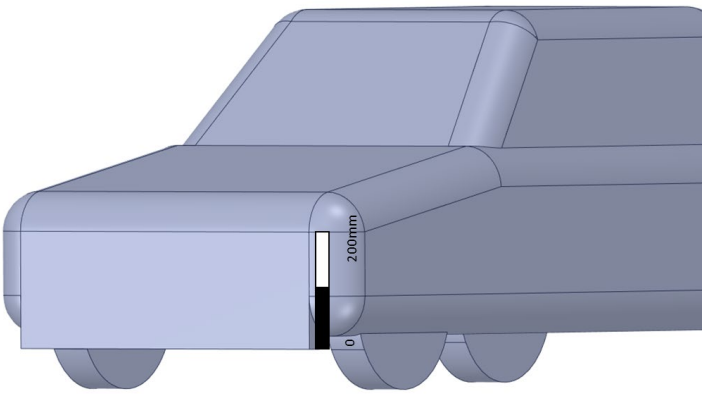

Figure 9 - Example of Front Air Dam added to Notchback Geometry

4.4.2 Front Air Dam Running

A number of issues occurred when initially running the simulations using the setting established for the notchback shape. As seen in Figure 9, the air dam has very harsh 90° angles at its lowest points. When trying to apply prism layer to this shape, the calculations did not fully complete, and an inaccurate flow structure consequently formed. By removing the prism layers around the air dam and increasing the underbody box mesh density, these issues were overcome and running continued without issue. Results were obtained for each air dam height, with lift and drag coefficients found and air pressure and velocity contours applied.

4.4.3 Rear Spoiler Study

The second aerodynamic element studied was a small rear spoiler. This is an element situated at the rear of the vehicle and designed to affect air flow over the top surfaces of the vehicle. CAD software Solidworks was utilised again to construct the rear spoiler (Figure 10), with differing heights produced again for comparison. The structure was then attached to the original notchback shape, and CFD simulations were performed using the settings in Table 5. The height of the spoiler varied from 25-50mm, with runs at 5mm intervals.

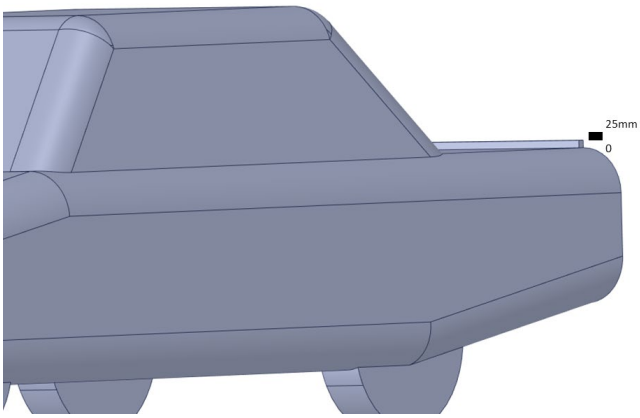

Figure 10 - Example of Rear Spoiler on the Notchback Geometry

4.4.4 Rear Spoiler Running

The running issues that occurred when testing the front air dam did not appear when running the different rear spoiler heights. Therefore, no changes were required to the initial software settings. Results were collated for the different spoiler heights, with lift and drag coefficients deduced, and pressure and velocity contour functions enabled in ANSYS.

5. Results

5.1 MIRA Geometries

By following steps detailed in Sections 4.2 and 4.3, comparison of lift and drag coefficients as well as air flow for the different MIRA reference shapes were collated.

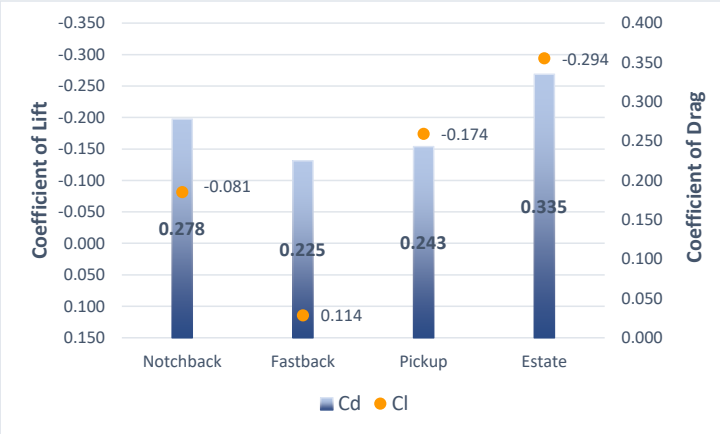

Figure 11- Mira Geometries Drag and Lift Coefficients. Drag Values are in bold.

The lift and drag coefficients for each of the MIRA shapes is displayed in Figure 11. As each of the shapes represents a generic version of a common automotive vehicle shape, testing the lift and drag can highlight patterns which could help avoid poor aerodynamic performance in the real world. Ideally, both lift and drag values should be as close to zero as possible to maximise aerodynamic efficiency. Of the shapes tested, the fastback is the most efficient in this regard, with drag and lift coefficients cumulatively only 0.339 away from zero. The notchback and pickup shapes are slightly less aerodynamically efficient, with cumulative lift and drag values of 0.359 and 0.417 respectively. Finally, the estate shape is the least aerodynamically efficient with cumulative lift and drag coefficients of 0.629. Looking at the coefficients separately, the notchback, pickup and estate all produce negative lift, with the notchback producing the lift value closest to zero out of the four shapes. The fastback shape is the only one to produce a positive lift value. The drag coefficients between the shapes are more similar to one another than the lift values, showing that altering the vehicle shape affects lift more than drag.

Finally, the estate shape, which sits much further from these ideal zero values, a whole 0.629 away from a perfect set of coefficient values. Whilst some negative lift can in theory

help with efficiency, it also comes with the pitfall of on-road instability. Therefore, the ideal values for both lift and drag sits at zero.

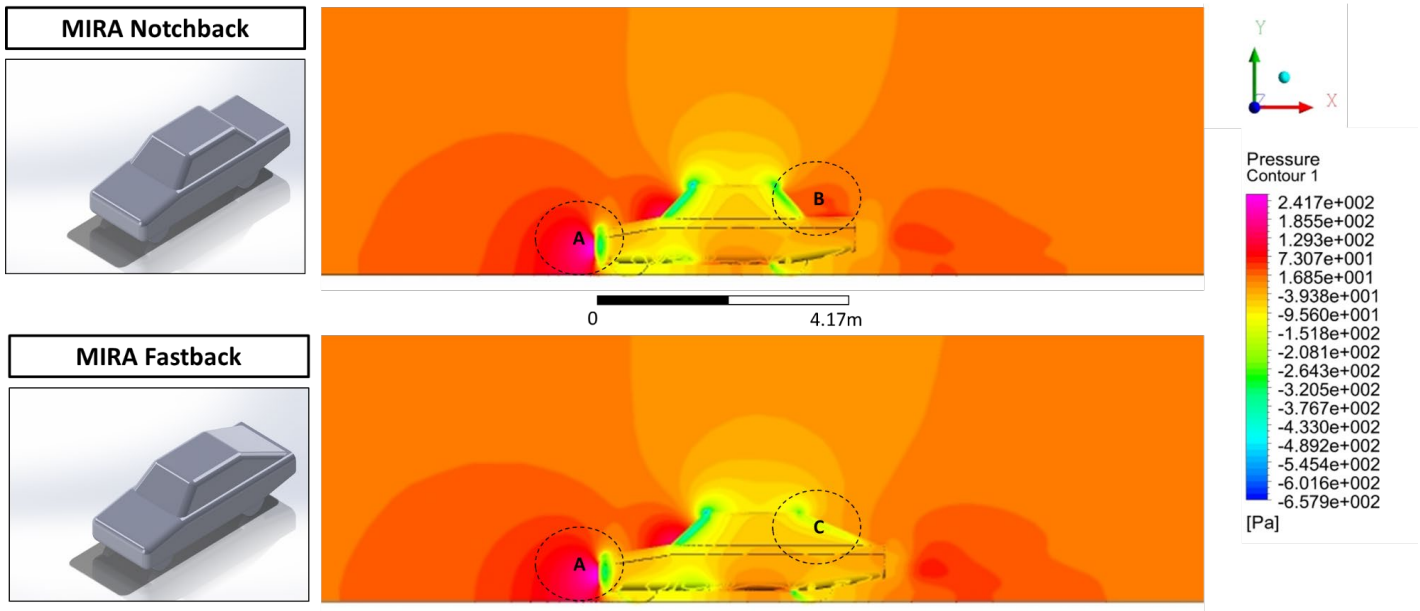

Figure 12 - Air Pressure contours, Notchback and Fastback.

Figure 12 shows the air pressure contours around both the notchback and fastback geometries, with an air velocity of 20m s^{-1} flowing from left to the right in each image. There is a comparable build-up of high pressure around the front of both geometries (Figure 12 (A)), which was as expected due to the identical front halves of the shapes. However, at Figure 12 (B) on the notchback a clear area of high pressure of approximately 1.685 $x10^1$ Pa can be seen where the rear window face falls away steeply. In contrast, at Figure 12 (C) on the fastback geometry, the rear window falls away at a lesser gradient which produces lower pressures of around -1.518 $x10^2$ Pa.

The differences in pressure front to rear of each geometry can be attributed to their respective drag values and help give an explanation as to why the fastback is subject to lower drag values than any of the other geometries.

The air pressure around the front of the pickup and estate is once again the same as the other geometries (Figure 13). Whilst neither the pickup or estate perform particularly efficiently, especially when considering lift, it is clear to see why the pickup is the more efficient of the two when looking at the pressure at the back of the vehicle. With both shapes, high pressure builds up much further behind the rear as seen in Figure 13 (A & B). In addition, Figure 13 (C) in both geometries displays a pressure formation of around -3.938 $x10^1$ Pa which could explain the high negative lift values produced by the two shapes when compared with the notchback and fastback. A cumulative lower air pressure is experienced over the top of the pickup and estate in comparison to the pressure experienced beneath each geometry.

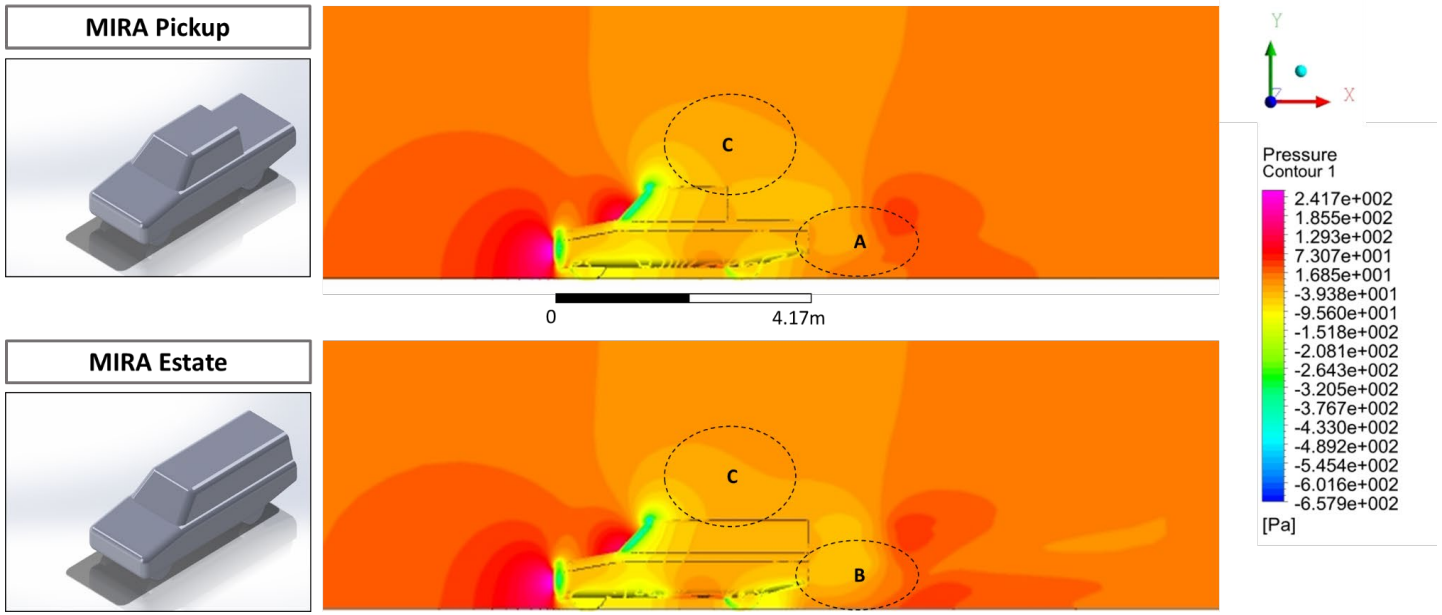

Figure 13- Air Pressure Contours, Pickup and Estate.

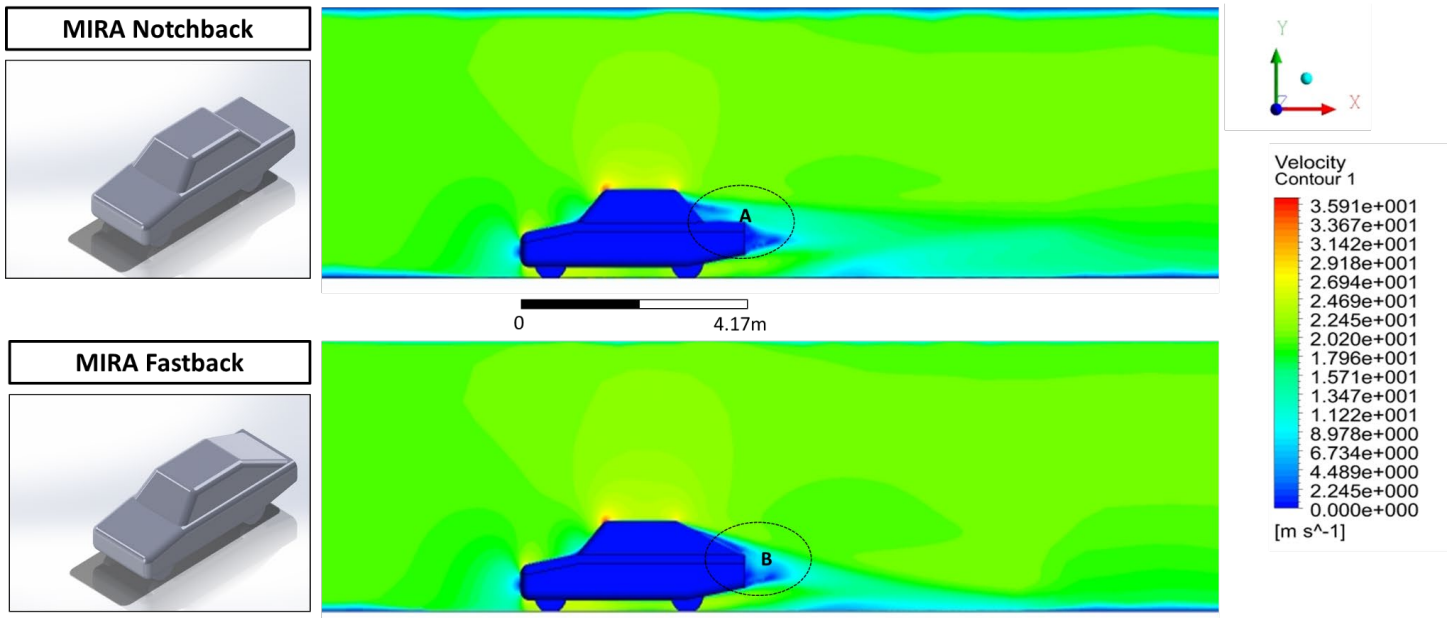

Figure 14- Air Velocity Contours, Notchback and Fastback.

In Figure 14 the air velocities around the notchback and fastback are displayed. The dark blue areas indicate very low air velocity, where the highest amount of turbulent air is present. Similar to the air pressure structures, no major differences are observed between velocities at the front of the geometries. There is however a distinct difference in air velocity at the rear of the geometries. In Figure 14 (A) two separate areas of highly turbulent air can be seen at the rear of the notchback. Figure 14 (B) however shows a single area of low velocity at the rear of the fastback shape, where near zero air velocity is far less prevalent.

Figure 15 displays air velocities around the pickup and estate geometries. One again, there is no difference between the velocity at the front of each vehicle. However, Figure 15 (A & B) highlight substantial differences in turbulent air flow at the rear. Both shapes produce much larger areas of low velocity air immediately behind the geometry than the notchback and fastback, and the extent of these near zero air velocity areas is much further behind the two geometries than those seen in Figure 14 (A & B). The increased turbulence at the rear of the pickup and estate likely contributed to the lift and drag coefficients seen in Figure 11. In addition, by comparing the air velocity and pressure contours over all the different geometries, a distinct relationship between areas of lower velocity and lower pressure can be seen.

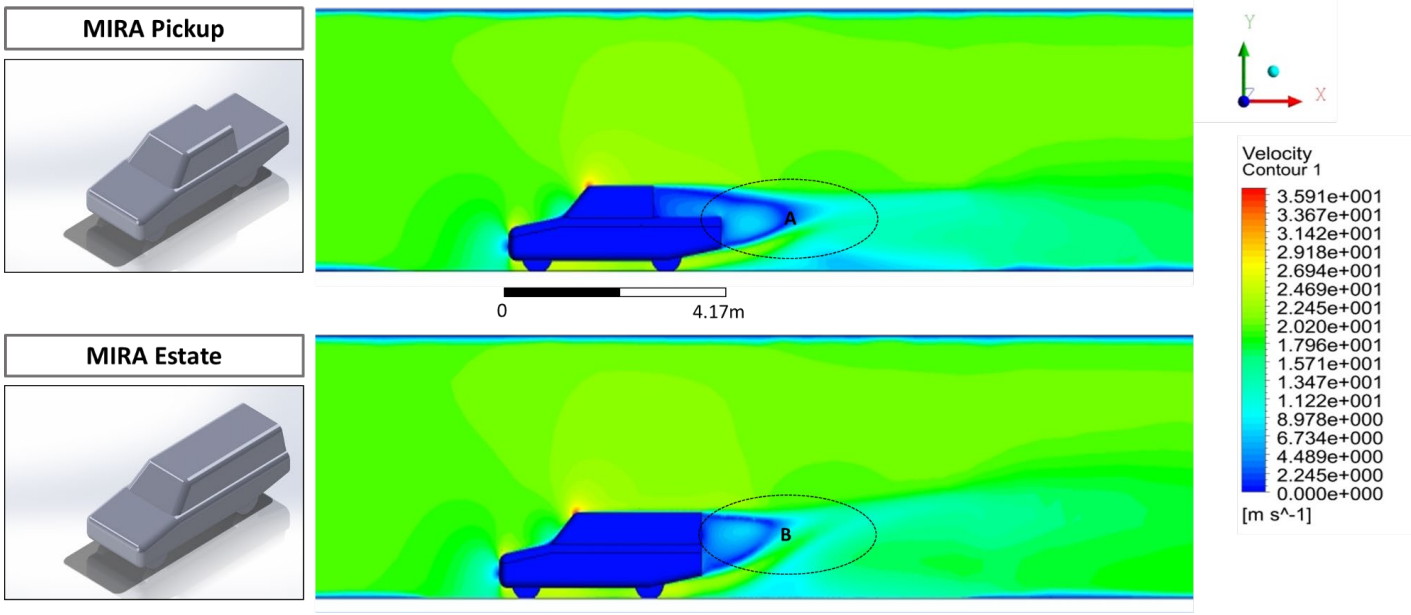

Figure 15- Air Velocity Contours, Pickup and Estate

5.2 Notchback Aerodynamic Components

5.2.1 Front Air Dam

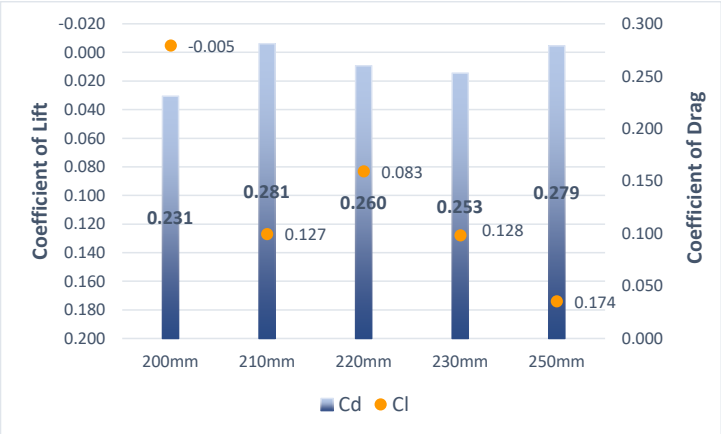

Figure 16- Front Air Dam Drag and Lift Coefficients.

Figure 16 presents lift and drag coefficients over a range of different air dam heights, ranging from 200m to 250mm. A front air dam is typically used to affect how quickly air flows underneath a vehicle, and thus how much pressure is present underneath the body. Ideally the coefficient of drag should be as near to zero as possible, as previously detailed in Section 5.1. However, an air dam is typically used as a performance aerodynamic component, therefore, the coefficient of lift should be as negative as possible. The more negative lift, the more downforce that is created which is often beneficial in performance vehicles. These negative values can transpire because in the equation for lift force (Section 3.2), the velocity and area will always be positive, thus, to produce a negative lift force a negative lift coefficient or negative pressure must be present. In the CFD simulations run here, the coefficient of lift is on occasion negative, meaning that negative lift forces are acting on the geometry at that point.

The 200mm air dam produced the least amount of drag, although all of the air dam heights were within 0.05 of the lowest value. Lift coefficients showed more variation, with the 200mm air dam the only one to generate negative lift. As the height of the air dam increased above 200mm, lift values sequentially increased away from zero, with the 220mm dam representing an exception to this.

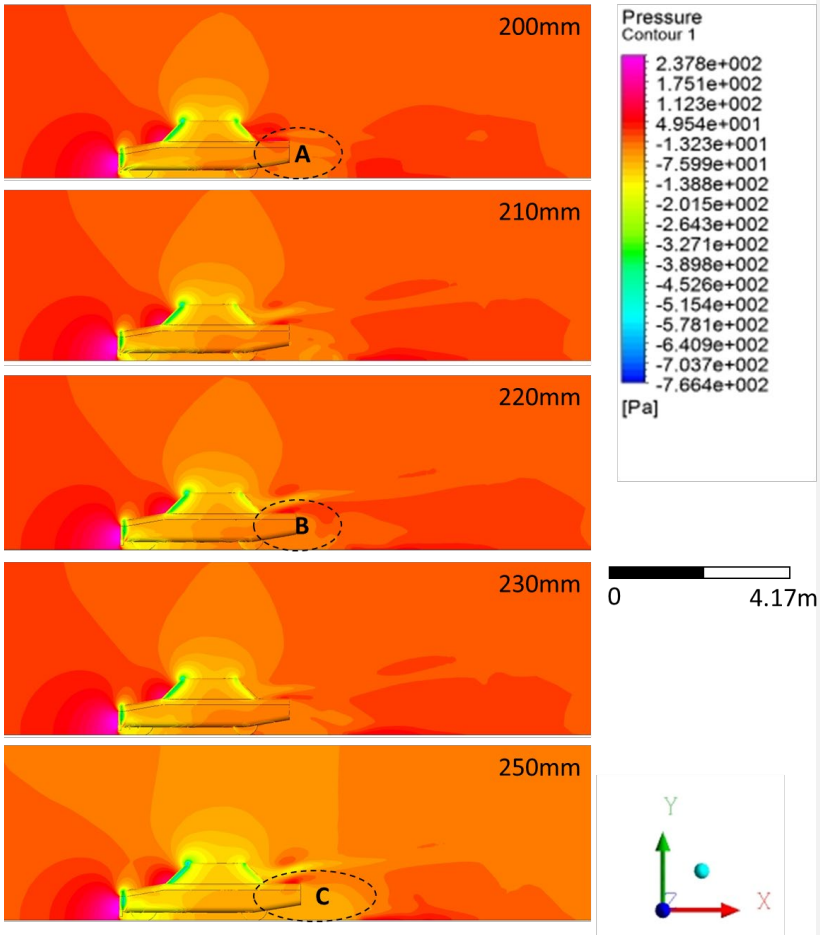

Figure 17- Air Pressure Contours, Front Air Dam.

When air pressure contours were added to the different air dams, variations in the air pressure around the rear half of the body can be seen despite the increments between heights being relatively small. In Figure 17 (A) on the 200mm air dam, the low pressure at the rear of the car relative to the front does not carry as far back as with the 220mm air dam at Figure 17 (B). Similarly, even greater lower pressure can be seen at the rear of the 250mm air dam geometry at point (Figure 17 (C)). Theoretically, as the air dam height is increased the pressure underneath and behind the car should become much lower, generating a greater difference in air pressure above and below the car, thus leading to more negative lift values.

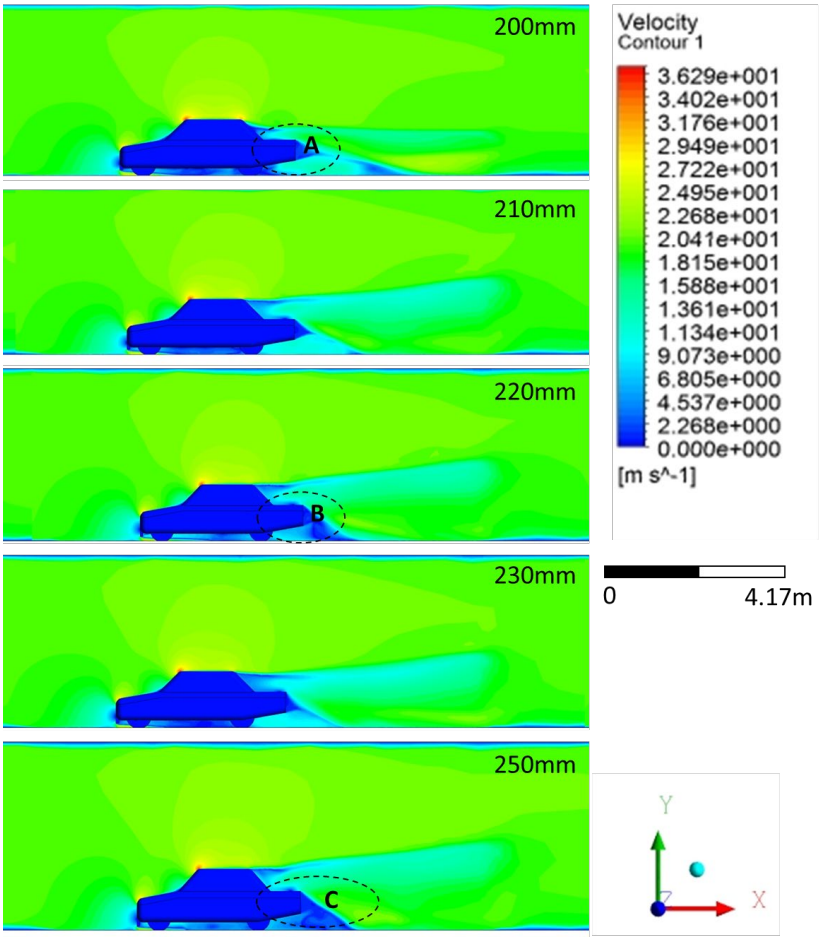

Figure 18- Air Velocity Contours, Front Air Dam.

Figure 18 shows the air velocity contours calculated from the simulation of air flow acting over the different air dam heights. As in Figure 17, changes in air velocity at the front of the geometry are relatively insignificant run to run. Conversely, air velocity fluctuations at the rear of each geometry are substantial. The 200mm air dam shows a very similar turbulence structure to that of the standard notchback geometry seen in Figure 14, with only a slightly larger area of low velocity below the rear of the geometry (Figure 18 (A)). At an air dam height of 220mm greater separation and turbulence can be viewed in Figure 18 (B) at the rear of the geometry, and this phenomenon becomes even more pronounced in Figure 18

(C). The largest air dam height produces a very large area of near zero velocity beneath the rear, extending further from the body also.

5.2.2 Rear Spoiler

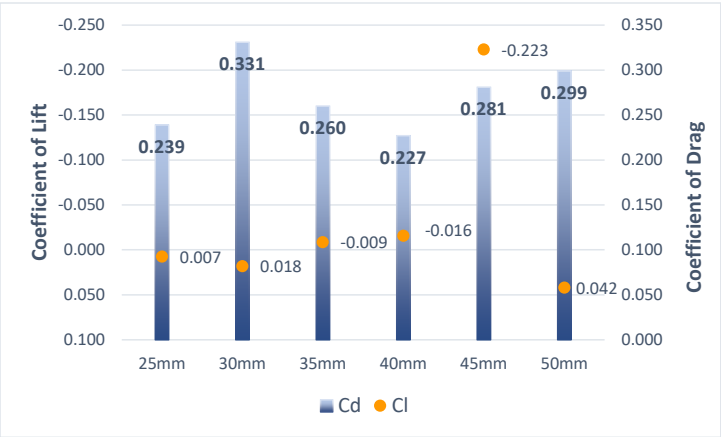

Figure 19- Rear Spoiler Drag and Lift Coefficients.

Figure 19 shows the drag and lift coefficients taken from 6 different rear spoiler heights tested in the ANSYS software. As with the front air dam, a rear spoiler is typically used to achieve enhanced aerodynamic performance as opposed to aerodynamic efficiency. Therefore, drag should be kept to a minimum whilst lift should be as negative as is possible. The ideal rear spoiler height should therefore simultaneously provide the most negative lift, whilst also attaining a drag coefficient that is nearest to zero.

The 40mm spoiler produces the coefficient of drag closest to zero, but similar to when the air dam was added, values only differ by a maximum of 0.104. The 40mm spoiler also produced negative lift, which was greater than that produced by the 35mm spoiler but less than the 45mm spoiler. The remaining spoiler heights all produced similar positive lift coefficients, ranging from 0.007 – 0.042. Therefore, the relationship between rear spoiler height and the lift and drag coefficients appears to be non-linear.

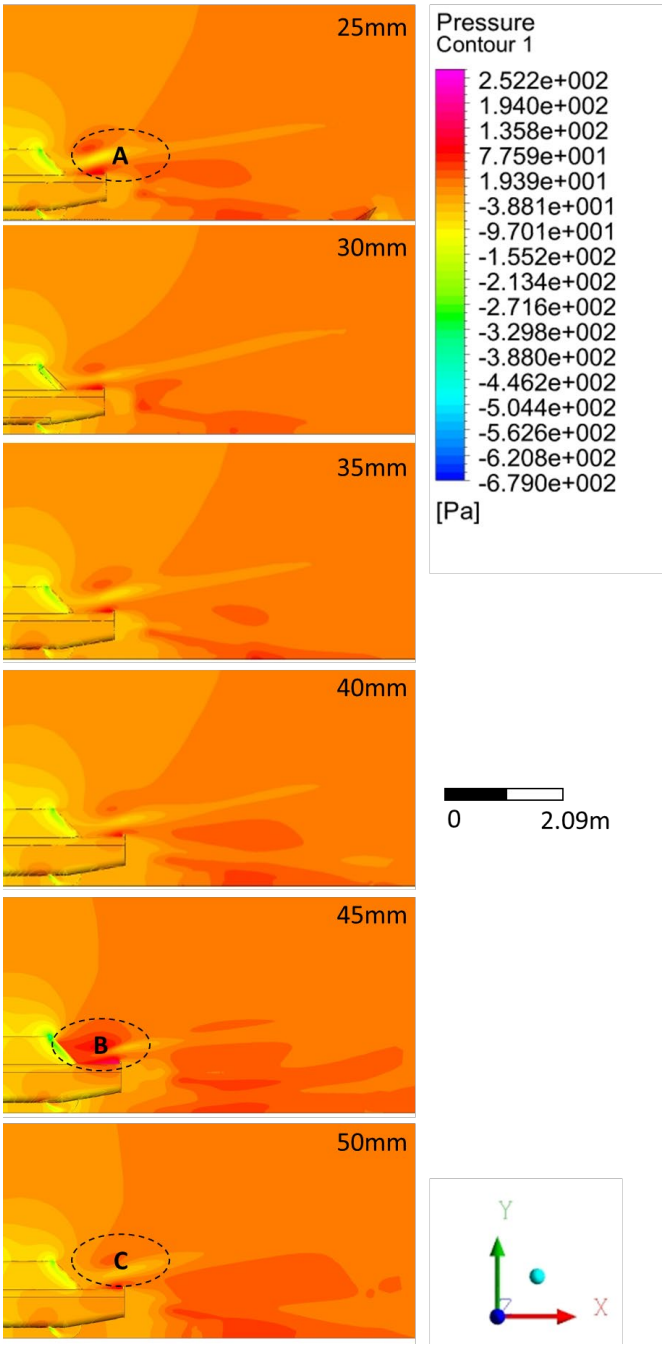

Figure 20- Air Pressure Contours, Rear Spoiler.

Air pressure contours for each rear spoiler height are displayed in Figure 20. Despite the rear spoiler only sitting at a height of 25mm, a disproportional difference in the pressure behind the geometry is seen in Figure 20 (A) when compared to the standard notchback running detailed in Figure 12. The area of pressure at the rear produced by the standard notchback geometry of approximately 1.685 $x10^1$ Pa changes with the 25mm rear spoiler addition, with a lance of negative pressure at around -9.701 $x10^1$ Pa intersecting this area. The addition of a 45mm rear spoiler creates a significant build-up of high pressure in front of the component (Figure 20 (B)) which leads to the greatest negative lift coefficient detailed in Figure 19. Finally, the 50mm spoiler does not yield such a drastic high pressure build up in front of the component yet does provide the greatest change in the angle of the low pressure coming off the rear of the geometry, as seen in Figure 20 (C).

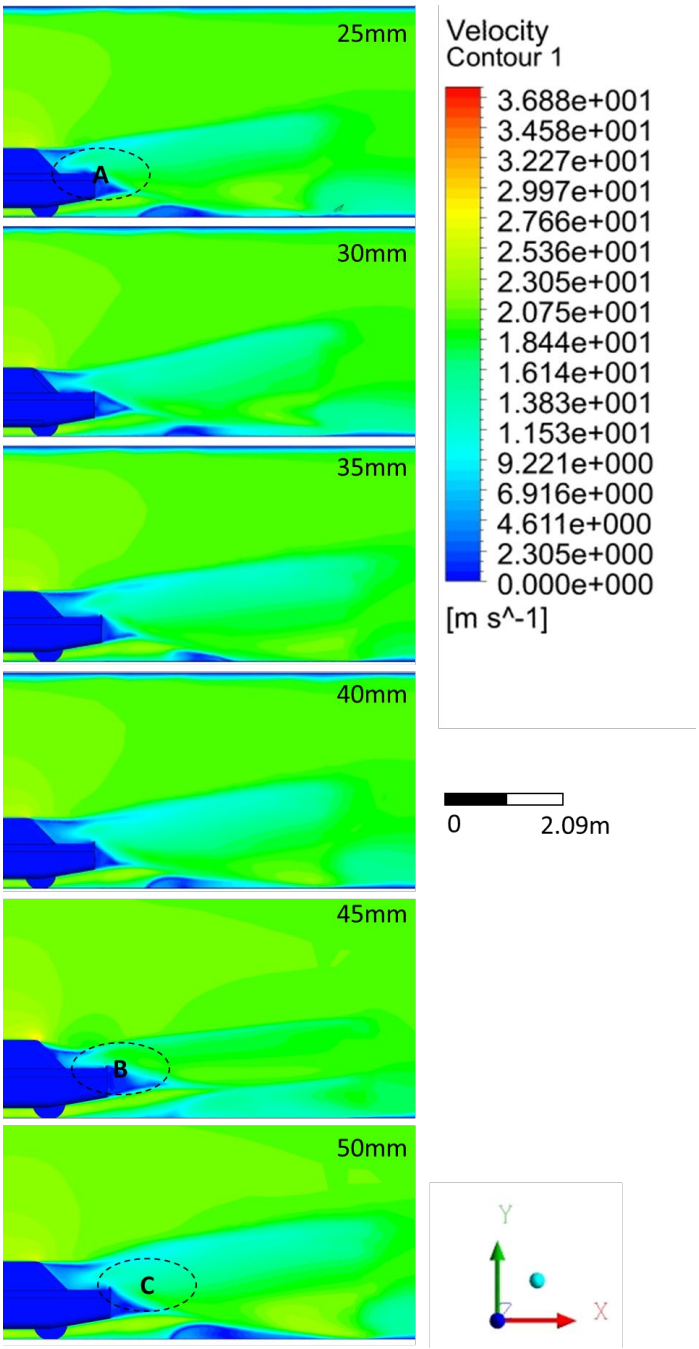

Figure 21- Air Velocity Contours, Rear Spoiler.

Figure 21 displays the air velocity contours acting over each of the different rear spoiler heights. As the spoiler height increases, an increase in air flow separation is observed at the rear of each geometry. The way in which the air flow separates behind the 25mm spoiler on Figure 21 (A), is very similar to the turbulent air flow observed behind the standard notchback geometry seen in Figure 13. In Figure 21 (B) an increase in turbulent, low velocity air flow can be observed behind he 45mm rear spoiler height. The largest of the rear spoilers at 50mm shows the greatest area of near zero air velocity behind the geometry and suffers the most from separation. This larger area of low velocity is seen in Figure 21 (C) and is likely the reason behind the 50mm rear spoiler having a greater coefficient of drag compared to some of the other rear spoiler heights.

6. Discussion

6.1 MIRA Geometries

Results outlined in Section 5.1. regarding each of the MIRA geometries were largely as expected, correlating well with previous work (Palaskar et al, 2016). The estate geometry was shown to be by far the least aerodynamically efficient of the vehicle shapes, whilst the pickup and notchback geometries showed similar levels of efficiency. The fastback was seemingly the most aerodynamically efficient geometry by some margin. The results seen can for the most part be attributed to how the rear of each geometry is modelled.

The results found largely match up with previous work completed on the same geometries (Banga et al, 2015) with a small percentage error experienced as was outlined in Section 4.2.3 in the methodology. As was expected, the estate geometry showed a substantially poorer level of aerodynamic efficiency over all of the other geometries. The pickup and notchback geometries were largely similar in respect to aerodynamic efficiency, with the fastback seemingly the most efficient by some margin. These results happen for the most part thanks to how the rear of each geometry is modelled.

The fastback geometry has the smallest angles running from the roof back down to the rear of the body. This lower angle allows for the airflow to remain attached to the surface of the body for longer, extending the boundary layer further back. As a result, air flowing over the vehicle can be kept close and remains mostly laminar in nature. This stability and lack of turbulent flow, relative to the other geometries, allows for a lesser difference in air pressures front to rear of the geometry. By producing this lower delta in pressure, the fastback has the lowest coefficient of drag. The lift is affected greatly by the efficiency with which air flow remains attached to this geometry. Figure 11 shows that the fastback is the only reference geometry producing a positive lift value. A lack of turbulence over the top of the body leads to a net lower pressure acting on the top of the body compared to the pressure acting on the under-side. This difference in pressure lifts the body up as more air flows over it.

All three of the remaining geometries react in a similar fashion, albeit at different magnitudes. Once again, the angle of the rear window section of each geometry is the most prominent cause of consequent lift and drag coefficient values. Visually, the notchback has less angle than both the pickup and estate geometries along the rear window face. However, the pickup geometry has characteristics far closer to the notchback. This can be attributed to the covered rear bed on the pickup. By having an elongated flat area before the rear of the body, a new boundary layer starts to form behind the initial turbulent flow caused around the middle of the body. A greater proportion of the air flow over the body then remains attached, thus causing more laminar flow around the rear of the body. The result of this is a much

Commented [EH7]: What do you mean by less angle. Hasn't the back roof got more angle as the pickup and estates are flat at the back?

lower difference in air pressure front to rear of the geometry compared to the estate geometry for example. If the bed on the pickup was open the separation over the top of the geometry would be more pronounced causing more drag. Additionally, the open bed itself would start acting similarly to a rear spoiler at the rear of the geometry, potentially generating more negative lift than previously seen.

Commented [EH8]: What would happen if it was an open bed pickup?

Finally, the estate geometry produces both the greatest drag coefficient and the most negative lift coefficient. This is due to how the air flow separates at the rear of the body. The 90-degree angle at the rear causes the air flow to very suddenly detach from the body causing a huge amount of turbulent flow. Consequently, the front to rear pressure delta is much larger than on any of the other reference geometries. The magnitude of the turbulent flow at the rear is so great that it also has a great effect on the lift coefficient of the geometry. Whilst not directly over the top of the vehicle, a large top to bottom pressure coefficient is experienced at the rear of the geometry. In this case, the pressure above the body is relatively higher in the turbulent air flow than underneath the body. This difference causes the geometry to get pushed in to the ground, a phenomenon regularly referred to as downforce.

Commented [EH9]: Thought this was good?

6.1.1 Relevance to the Modern Automotive Design Process

The key focus of this project is to determine how relevant MIRA reference geometries can be to real-world automotive design processes. Whilst all of the geometries do show accurate flow structures and values for lift and drag, the physical shapes are both flawed in places and outdated in the modern world of automotive design. The most pressing issue regarding all of the geometries is how harsh almost all of the air flow critical angles are. This is at its most prominent on the estate geometry. By having a sheer 90-degree angle at the rear, huge amounts of turbulent flow are produced, which highlights a critical issue with this MIRA geometry. Automotive companies have long since understood and compensated for this particular issue, with most estate vehicles designed with long, swept back rear ends more akin to the rear window angles seen on the fastback geometry. Similar issues are prevalent across all of the MIRA geometries, with the very angular shapes not holding any resemblance to modern designs of the same vehicle types. Consequently, the MIRA reference geometries in their current form can add little to the modern automotive design process.

Another key geometry issue present across all of the MIRA reference geometries is that of the rear underbody design. A prominent angle can be seen between the rear wheels and rear end of each geometry. This causes the air to flow more quickly under the vehicles and

at their rears, causing a great deal of negative lift across all the geometries, with the fastback the only exception thanks to a more efficient overall design. As most automotive designs aim for neutrality, a disruptive feature such as this which promotes negative lift is not something that most standard vehicles would have design in. Added to the issues with the angular nature of the geometries, the relevance to the modern design process is further diminished.

Therefore, it is clear that, whilst still extremely valuable for software calibration and academic use, the MIRA reference geometries are not relevant to the modern automotive design process.

6.1.2 Potential Improvements

Having recognised the limitations of the MIRA reference geometries in their current form with regards to informing modern automotive design processes, certain aspects could easily be improved or adjusted to allow the reference geometries to become more relevant. Firstly, changing the geometries to have less aggressive angles and a more practical underbody shape and design would make a huge difference. By employing shapes more reminiscent of modern vehicles as opposed to the current geometries, which sit much closer to designs from the 1960s and 1970s, relevance to modern design would increase.

Another area in which the MIRA reference geometries fall short in regard to being a design aide is the range of shapes available. The current automotive world is full of hatchbacks, MPVs, SUVs and crossovers, all of which produce air flow characteristics that are not well represented by the current MIRA geometries. Through adding a set of newer updated shapes, the MIRA geometries could be useful not only for calibration and academic purposes, but also as a suitable platform for testing new development and design ideas in an efficient and cost-effective way.

6.2 Notchback Aerodynamic Components

6.2.1 Front Air Dam

A front air dam is a rudimentary aerodynamic performance element and as such, is designed to produce a certain amount of negative lift to improve speed and handling performance in cornering situations. The rear of all of the MIRA geometries has an angled “diffuser” of sorts that causes a certain level of negative lift. Because of this feature the front air dam does not have the desired effect. The shape at the rear of the notchback causes the air further forward to stall under the vehicle and move slowly which is not the intended outcome. Ideally, the deflection of air caused by the front air dam should increase the speed of the air flow underneath the vehicle and decrease pressure, whilst doing the opposite across the top

surfaces of the vehicle. However, the stalled air underneath the vehicle in this particular case causes a delta of pressure in the opposite direction and thus, causes positive lift instead of the anticipated negative lift.

Changing certain elements of the MIRA reference geometries could well improve upon their relevance to real world design and development. For example, by introducing a flatter underside or a more common, lower ride height, the front air dam would most probably act as expected. In the case of a front air dam, the extensive history and success of the component and its implementation allow for knowledge of what should be expected. The testing carried out as a part of this project shows how, in their current state, the MIRA reference shapes do not suitably accommodate the successful CFD testing of a front air dam.

6.2.2 Rear Spoiler

The rear spoiler testing provided results much closer to reality than those produced by the front air dam. The reversed and turbulent air flow that builds up in front of each rear spoiler provides a new surface for air flow to attach to and, generally speaking, more negative lift values are formed compared to the standard notchback geometry. Once again, the results are not completely consistent, and this is due to the design of the MIRA reference geometry. With the angle at the rear of the geometry already producing a certain level of negative lift as previously described, some of the lower rear spoiler heights do not improve the negative lift values from the standard shape, but instead increase drag. The 35mm through to the 45mm rear spoilers produce exactly what would be expected of a rear spoiler. The 50mm spoiler should, in theory continue this trend, but the results are seemingly erroneous and thus an unknown issue must have hampered the simulation.

As with the front air dam, the design of the standard MIRA notchback causes the results to vary from expectation. By implementing the same changes suggested in the previous section, a more consistent set of results could be obtained and a greater relevance to real-world aerodynamics would be attained.

6.2.3 Relevance to Real-World Aerodynamic Development

With both the front air dam and rear spoiler studies a number of issues with the MIRA reference geometries are highlighted when being used as a test bed for aerodynamic elements. The rear spoiler was by far the more successful of the two elements tested, because whilst simplistic, the shapes on the top of the MIRA notchback are not the cause of any particular aerodynamic effects. Effects such as the improved boundary layer produced

Commented [EH10]: what do you mean by this?

by the underside diffuser angle also present on the notchback geometry. Conversely, with the front air dam the underside of the notchback is crucial and the strange diffuser at the rear causes a set of results that do not line up with expectations at all. Small changes could very quickly improve how this particular reference geometry reacts to added aerodynamic elements.

7. Conclusion

Having completed CFD running on all of the MIRA geometries it is clear that, as a modern automotive design aid, the shapes are somewhat outdated. The angular form on all of the shapes cause far more turbulence that would typically be seen on more modern vehicle designs. In addition, the underbody design on all of the MIRA reference geometries cause a certain amount of downforce. Whilst that is not necessarily a bad thing to produce, road cars are more typically focused on neutrality of handling and economic performance. Downforce typically works against both of those concepts. Rounding off of angles and potential additional geometries would drastically improve upon how relevant the MIRA geometries could be to the modern automotive design process. In their current state however, the shapes used represent a much older design than would currently be seen on the roads.

Both the front air dam and rear spoiler studies suffered from the unique underbody design found on the MIRA reference geometries. The front air dam study outputted results that almost entirely went against what would be expected from the addition of a front air dam. Whilst the rear spoiler study fared better in this respect, a negative affect was still felt from the rear end design of the MIRA notchback. In conducting these studies, it is evident that to a good extent the MIRA geometries allow for a reasonable visualisation of certain air flow structures produced by aerodynamic elements on the upper surface of the body, such as a rear spoiler. Underbody components are much more directly affected by the MIRA geometry design and thus gathering any meaningful results from aerodynamic components in that area is an unreasonable goal. Moreover, the flattening of the underbody of the MIRA reference geometries would help overcome this issue and so, at least for providing a proof of concept or basic understanding of any given aerodynamic component, would become much more useful.

Having completed a large amount of CFD simulation running using shapes and aerodynamic designs that are well documented on, the results were predominantly successful with only one or two runs proving to be erroneous in nature. The main aim for this project was to determine how relevant and useful the MIRA geometries currently are to the design process in the automotive industry. As a result, it can be shown that these geometries in their current forms simply do not suitably replicate real-world designs, and thus are not suitable for use as an aid to the automotive design process. However, the way in which the results and initial calibration lines up with the extensive literature already surrounding the MIRA geometries, does show just how valuable the MIRA reference geometries are for both calibration and academic purposes.

In closing, this project has shown conclusively that as a part of the design process these MIRA reference geometries are not up to the task. With very small changes these geometries could be used as a proof of concept for aerodynamic components. Further work and additional new vehicle shapes could also make the geometries useful to the design process in an automotive context and allow for uses of the MIRA geometries outside of their achievable current scope.

8. Recommended Further Work

8.1 Small Scale Wind Tunnel Testing

Further calibration and validation of the MIRA notchback was conducted as a part of this project, with time constraints eventually leaving it out of the main body of work.

By taking a 3D printed model of the notchback geometry and placing it within a small-scale wind tunnel in the IQ building on campus at UWTSD Swansea, further exploration of air flow structures could be conducted. In addition, both lift and drag coefficient values could be calculated from this running which could further validate the in-simulation CFD calibration conducted. Whilst in a small wind tunnel the physical lift and drag forces may differ from a full one to one representation of the geometry, the coefficients of both lift and drag would be comparable.

Commented [EH11]: Do you need to say this?

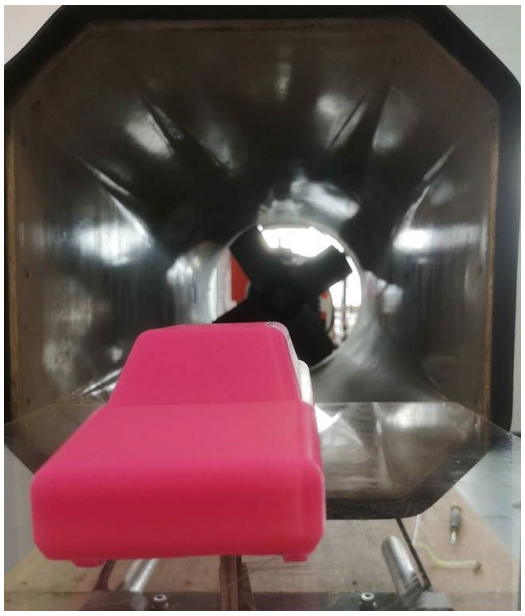

Figure 22 - 3D Printed MIRA Reference Geometry in Small Scale Wind Tunnel.

Figure 22 shows the printed model in the wind tunnel as a part of some initial running. Further set up was required and unfortunately, was not completed in time to be a main part of this project.

8.2 Increased Scope

If funding, resources and time were not limited, a much more extensive regime of calibration and testing could have complemented this project. The aforementioned wind tunnel for example could be upscaled to a full-size model and wind tunnel so as to attain real-world values for each stage of testing. Producing one to one scale models of each geometry and also the different aerodynamic elements could further prove how each scenario relates to the real-world.

Additionally, more aerodynamic elements could be tested to see how they react to the unique shape of the MIRA geometries. It could further highlight how the MIRA shape interferes with expected air flow structures, particularly with more underbody components such as side skirts or a more complex diffuser design built around the existing shape. With newer improved computing systems and increased computing power, much more calibration could be completed and a greater deal of extensive and more accurate running accomplished.

8.3 MIRA Reference Redesign

A key aspect of the discussion and analysis of the results described potential ways in which the geometries could be changed and brought in to line with more modern design conventions. With more time, potentially as a subsequent project leading on from this one, the geometries could be redesigned and expanded upon. Inclusion of more shapes, such as a hatchback, based upon mass produced examples, such as the incredibly popular Ford Fiesta, could well be beneficial and further expose how aerodynamic efficiency changes between vehicle shapes. Optimization of the MIRA reference geometries is something that other studies have explored (Zhang et al, 2014). Applying knowledge from these sources and considering real-world automotive design could allow for a complete reimagining of the MIRA reference geometries. Providing a generic test bed, not only for design purposes, but also the existing calibration purposes is the natural next step for the conducted research in this project to take.

Commented [EH12]: Such as?

9. References

1. Abdel-Rahman, A., Agelin-Chaab, M., Elfstrom, G. and Komar, J., 2016. *Integrated Aero-Thermal Testing of a Race Car in a Full Scale Climatic Wind Tunnel* (No. 2016-01-1588). SAE Technical Paper.
2. Altinisik, A., 2017. Aerodynamic Coastdown Analysis of a Passenger Car for Various Configurations. *International Journal of Automotive Technology*, *18*(2), pp.245-254.
3. Banga, S., Zunaid, M., Ansari, N.A., Sharma, S. and Dungriyal, R.S., 2015. CFD Simulation of Flow Around External Vehicle: Ahmed Body. *Journal of Mechanical and Civil Engineering*, *12*(4), pp.87-94.
4. Cambridge Dictionary, 2019. *Aerodynamics.* [Online] Available at: https://dictionary.cambridge.org/dictionary/english/aerodynamics [Accessed on 12/1/2019].
5. Chainani, A. and Perera, N., 2008. 'CFD Investigation of Airflow on a Model Radio Control Race Car', *Proceedings of the World Congress on Engineering 2008*, 2-4 July. London.
6. Cyr, S., Ih, K.D. and Park, S.H., 2011. *Accurate Reproduction of Wind-tunnel Results with CFD* (No. 2011-01-0158). SAE Technical Paper.
7. Darling, D., 2016. *Opel-RAK.* [Online] Available at: http://www.daviddarling.info/encyclopedia/O/Opel-RAK.html [Accessed 2/2/2019].
8. Dietz, K. and Heesterbeek, J.A.P., 2002. Daniel Bernoulli's epidemiological model revisited. *Mathematical biosciences*, *180*(1-2), pp.1-21.
9. Earl, C.C., 1947. *Investigation into the Development of German Grand Prix Racing Cars Between 1934 & 1939.* HM Stationary Office, London.
10. Fluent User Services Centre, 2006. *Introductory FLUENT Notes: FLUENT v6.3.* [Online] Available at: http://www.southampton.ac.uk/~nwb/lectures/GoodPracticeCFD/Articles/Turbulence_Notes_Fluent-v6.3.06.pdf [Accessed on 1/4/2019].
11. Gaylard, A.P., Baxendale, A.J. and Howell, J.P., 1998. *The Use of CFD to Predict the Aerodynamic Characteristics of Simple Automotive Shapes* (No. 980036). SAE Technical Paper.
12. Gaylard, A.P., Howell, J.P. and Garry, K.P., 2007. *Observation of Flow Asymmetry Over the Rear of Notchback Vehicles* (No. 2007-01-0900). SAE Technical Paper.
13. George, B., 2014. 'Aerodynamic Designing and Position Optimization of Roof Box'. MSc by Research Thesis. Coventry University, Coventry.

14. Ghita, M.C., Micu, A.C., Talu, M.D. and Talu, S.D., 2012. Shape Optimization of Vehicle's Methane Gas Tank. *Annals of the Faculty of Engineering Hunedoara*, *10*(3), p.259.
15. Gibbs-Smith, C.H., 1962. *Sir George Cayley's Aeronautics, 1796-1855*. HM Stationery Office, London.
16. Govardhana, M. and Reddy, B.V., 2014. Estimation of Drag and Lift on Ahmed Body Using CFD Analysis. *Journal of Advanced and Innovative Research, 3(8),* pp.51-55.
17. Groover, M. and Zimmers, E.W.J.R., 1983. *CAD/CAM: Computer-Aided Design and Manufacturing*. Pearson Education, New Jersey.
18. Heft, A.I., Indinger, T. and Adams, N.A., 2012. *Introduction of a New Realistic Generic Car Model for Aerodynamic Investigations* (No. 2012-01-0168). SAE Technical Paper.
19. Howell, J., Passmore, M.A. and Tuplin, S., 2013. Aerodynamic Drag Reduction on a Simple Car-like Shape with Rear Upper Body Taper. *SAE International Journal of Passenger Cars – Mechanical Systems, 6(1),* pp.52-60.
20. Jakab, P.L., 2014. *Visions of a Flying Machine: The Wright Brothers and the Process of Invention*. Smithsonian Institution, Washington.
21. Katz, J., 1995. *Race Car Aerodynamics: Designing for Speed,* 2nd edn. Bentley Publishers, Massachusetts.
22. Katz, J., 2006. Aerodynamics of Race Cars. *Annual Review of Fluid Mechanics*, *38*, pp.27-63.
23. Lanfrit, M., 2005. *Best Practice Guidelines for Handling Automotive External Aerodynamics with FLUENT*. Fluent Inc, Germany.
24. Le Good, G.M., Howell, J.P., Passmore, M.A. and Cogotti, A., 1998. A Comparison of On-road Aerodynamic Drag Measurements with Wind Tunnel Data from Pininfarina and MIRA. *SAE transactions*, *107,* pp.967-976.
25. Lienhart, H., Stoots, C. and Becker, S., 2002. Flow and Turbulence Structures in the Wake of a Simplified Car Model (Ahmed Model). In *New Results in Numerical and Experimental Fluid Mechanics III* (pp. 323-330). Springer, Berlin.
26. McBeath, S., 2015. *Competition Car Aerodynamics: A Practical Handbook*. Veloce Publishing, Dorset.
27. Musa, J.K. and Patel, P.D., 2016. Aerodynamic Drag Reduction of a Passenger Vehicle by Controlling the Wake using CFD Analysis. *International Journal of Science Technology & Engineering, 2(11),* pp.282-288.
28. Palaskar, P.M., Kumar, V. and Vaidya, R., 2016. *Methodology Development to Accurately Predict Aerodynamic Drag and Lift for Passenger Vehicles Using CFD* (No. 2016-01-1600). SAE Technical Paper.

29. Parab, A., Sakarwala, A., Paste, B., Patil, V. and Mangrulkar, A., 2014. Aerodynamic Analysis of a Car Model Using Fluent-Ansys 14.5. *International Journal On Recent Technologies On Mechanical and Electrical Engineering, 1(4),* pp.7-13.
30. Posthumus, C. and Tremayne, D., 1985. *Land Speed Record: From 39.24 to 600+ MPH.* Osprey, London.
31. Sharma, R.B. and Bansal, R., 2013. CFD Simulation for Flow Over Passenger Car Using Tail Plates for Aerodynamic Drag Reduction. *Journal of Mechanical and Civil Engineering*, *7*(5), pp.28-35.
32. Soares, R.F. and de Souza, F.J., 2015. *Influence of CFD Setup and Brief Analysis of Flow Over a 3D Realistic Car Model* (No. 2015-36-0513). SAE Technical Paper.
33. Zhang, X., Toet, W. and Zerihan, J., 2006. Ground Effect Aerodynamics of Race Cars. *Applied Mechanics Reviews*, *59*(1), pp.33-49.
34. Zhang, Y., Ding, W. and Zhang, Y., 2014. *Aerodynamic Shape Optimization Based on the MIRA Reference Car Model* (No. 2014-01-0603). SAE Technical Paper.
35. Zhang, Y., Zhang, Z., Li, J., Shao, S. and Guo, S., 2013. *Test Process and Correction of Automotive Wind Tunnel in Jilin University China* (No. 2013-01-1351). SAE Technical Paper.